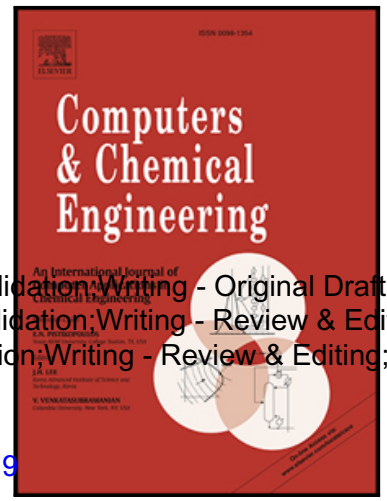

Predictive Two-Phase Modeling and Improvement for Industrial Unipol® Polypropylene Process – Development and A Case Study

Eslam S. Sbaaei Methodology;Investigation;Formal analysis;Software;Validation;Writing - Original Draft;Visualizati
Mai M. Kamal Fouad Conceptualization;Methodology;Formal analysis;Validation;Writing - Review & Editing;Visuali
Tamer S. Ahmed Conceptualization;Methodology;Formal analysis;Validation;Writing - Review & Editing;Visualizatio

PII: S0098-1354(19)31123-8
DOI: https://doi.org/10.1016/j.compchemeng.2019.106719
Reference: CACE 106719

To appear in: *Computers and Chemical Engineering*

Received date: 25 October 2019
Revised date: 24 December 2019
Accepted date: 29 December 2019

Please cite this article as: Eslam S. Sbaaei Methodology;Investigation;Formal analysis;Software;Validation;Writing -
Mai M. Kamal Fouad Conceptualization;Methodology;Formal analysis;Validation;Writing - Review & Editing;Visuali
Tamer S. Ahmed Conceptualization;Methodology;Formal analysis;Validation;Writing - Review & Editing;Visualizatio
Predictive Two-Phase Modeling and Improvement for Industrial Unipol® Polypropylene Process – Development and A Case Study, *Computers and Chemical Engineering* (2019), doi: https://doi.org/10.1016/j.compchemeng.2019.106719

Highlights:

- A two-phase model for industrial Unipol® polypropylene plant is presented using Aspen Plus
- Industrial data were used for model calibration and validation
- The model was used for studying process variables and in process improvement.
- The improvement illustrated a remarkable savings in energy consumption while enhancing the plant throughput.

Predictive Two-Phase Modeling and Improvement for Industrial Unipol® Polypropylene Process – Development and A Case Study

Eslam S. Sbaaei [a], Mai M. Kamal Fouad [a], Tamer S. Ahmed [a, b]*

[a] Chemical Engineering Department, Faculty of Engineering, Cairo University

Giza 12613, Egypt

[b] Environmental Engineering Program, Zewail City of Science and Technology, 6th of October City, Giza 12578, Egypt

* Corresponding author: Tel.: +20 114 292 4407

E-mail address: Tamer.S.Ahmed@cu.edu.eg (Tamer. S. Ahmed)

Abstract

This work presents a two-phase model describing propylene catalytic polymerization for Unipol® technology with a fluidized bed reactor (FBR) using Aspen Plus® software and the sequential modular simulation approach. The hydrodynamic aspects of the FBR were incorporated to provide better realism in describing the performance of the FBR. A detailed kinetic multi-site model for polymerization reactions occurring inside the FBR was proposed. Industrial data from a Unipol® plant during normal operation were used to calibrate the model parameters. Obtained data sets were tested and screened to confirm data validity for establishing the model and averting incorrect outcomes. The model was validated against different industrial data and then was used to investigate the influences of different process variables on the plant's performance. Finally, the model was used to improve the process

illustrating a prospective for remarkable savings in energy consumption in the process while enhancing the plant throughput.

Keywords: Unipol Technology; Polypropylene; Aspen Plus; Fluidized Bed Reactor; Sequential Modular Simulation.

1. Introduction

The worldwide Polypropylene (PP) demands are remarkably increasing as a consequence of the diversity in its morphological structures and the superiority in its characteristic properties (Biron, 2018). Since its discovery, polypropylene has been gained enormous popularity rapidly among commodity plastic materials. The most realistic cause for this success is its combination between low costs and impressive mechanical properties, which make it better than polyethylene (Maddah, 2016). With the development of new technologies for polypropylene production, its applications have expanded rapidly to all fields, taking advantage of its unique characteristics to produce flexible, long-lasting, low-priced and light plastics for plentiful industrial, commercial, medical, and personal purposes.

Various reliable and versatile process technologies such as Hypol®, Novolen®, Innovene®, Spheripol®, Catalloy® and Unipol® have been designed to produce different grades of polypropylene meeting the market requirements for the most demanding applications (Luo et al., 2009). Nevertheless, Unipol® technology is one of the prevailing choices for polypropylene production. This technology relies substantially on a fluidized bed reactor (FBR) in which a gas-phase polymerization process occurs. In contrast to other technologies' reactors, the numerous advantages of gas-phase FBR, such as its ability to carry out a variety of multiphase chemical reactions, good contact and mixing between reactants, no need for solvent, higher mass and heat transfer rates, better heat removal, and lower

operating conditions with continuous and steady-state operational modes, have made it one of the most widely utilized reactors in chemical industries, particularly in the polymerization field (Jafari et al., 2004a; Shamiri et al., 2011). However, compared to other industrial gas-solid reactors such as fixed and moving bed reactors, the hydrodynamic natures of FBRs is much more complex.

The literature have reported different mathematical models for characterizing the hydrodynamic performance of industrial FBRs (McAuley et al., 1990; Choi and Ray, 1988; Hatzantonis et al., 2000; Ibrehem et al., 2009). The hydrodynamic models reported can be divided into four general categories, i.e., single-, two-, three- and four-phase models. However, the two-phase concept is the prevailing to characterize the fluidization phenomena inside industrial FBRs. In reality, the fluidized bed of these reactors may run at several fluidization regimes, i.e. bubbling, slugging, turbulent and fast fluidization regimes, according to its operating conditions. None of these regimes is satisfactory to meticulously represent the perfect performance of the fluidized bed during operation (Mostoufi et al., 2001). Typically, the fluidization of the FBR bed during regime-transition may exhibit different flow regimes. Nonetheless, the hydrodynamic two-phase model and the generalized bubbling/turbulent model are both applicable at these different fluidization regimes (Jafari et al., 2004b).

Mathematical models have been adopted based on many hypotheses and approximations to what is happening practically within the industrial FBRs. Normally, these approximations are submitted to simplify the complexity of the empirical equations utilized to describe the hydrodynamic natures of these reactors (Hatzantonis et al., 2000; Shamiri et al., 2010; Kiashemshaki et al., 2006). However, since there is no definitive FBR mathematical model that can describe entirely the actual FBR performance, some of the results of these models are somewhat paradoxical. For the developed model to be applicable in plant design, process

optimization and control, …, etc., a tight linkage among all simulating aspects is required. Thus, a reliable model for the polymerization process that can describe physical and thermodynamic properties, phase equilibrium, and polymerization kinetics is prerequisite for exploring the influence of fluctuations in feeding composition, operating conditions and even process variables during plant operation (Luo et al., 2009; Khare et al., 2002; 2004; Zheng et al., 2011).

Although many of the simulating aspects of polymerization can be considered using commercial process simulation programs such as Aspen Plus software (Polymer Plus®), the number of models offered in the literature is much lower than mathematical models. The main reason is the lack of direct simulating tools in these commercial simulators to simulate the complex FBR hydrodynamics. This prompted model developers to resort desirously to mathematical modeling to simulate the hydrodynamic characterizations of industrial FBRs, and thus giving these models the priority in application. However, through commercial Aspen Plus software, the developed models can elucidate seamlessly the physical and thermodynamic properties, catalyst characteristics, and polymer specifications, as well as the single and multiple-site traditional Ziegler-Natta (Z-N) polymerization kinetics.

Khare et al. (2002, 2004) developed a steady-state and dynamic Polymer Plus® model for gas phase polypropylene process and slurry high density polyethylene process using CSTRs. In addition, Luo et al. (2009) described the strategy of modeling by Aspen Plus software for the polypropylene process based on Hypol® technology. They focused on the thermodynamic understanding and accurate modeling of the polymerization reactors with non-equilibrium behavior. Otherwise, Zheng et al. (2011) performed a steady-state and dynamic modeling by Polymer Plus® for the Basell multi-reactor olefin polymerization process of Spheripol® technology. However, all these erstwhile investigations neglected the hydrodynamic influences during developing their models. Furthermore, they dealt with the fluidized bed as

operating in a well-mixed (single phase) regime in case of gas-phase polymerization and in a plug-flow (single phase) regime in case of liquid-phase polymerization. This decreases the feasibility of these models over wide range of operating conditions. On the other hand, although a two-phase FBR model was considered to simulate the fluidized bed in its actual fluidization regime (Shamiri et al., 2010; 2011; Abbasi et al., 2016; Mahecha-Botero et al., 2009), it was not considered in the literature using Aspen Plus software.

In this work, a steady-state two-phase modeling for industrial bulk polypropylene process of Unipol® technology using Polymer Plus® and the built-in sequential modular simulation (SMS) approach with the hydrodynamic correlations is presented. The SMS approach technique allows the key hydrodynamic parameters to contribute in the model development, providing a more realism during describing the performance of industrial FBRs. In addition, incorporating this approach into Polymer Plus® allows the model to deal with more than one fluidization regime as in these reactors. This approach has been used to meticulously simulate the actual performance of an industrial FBR of an existing Unipol® plant. Moreover, the current work presents an advanced iterative methodology supported by Aspen Plus Optimizer® tool to calibrate the kinetic parameters of the multisite Z-N catalyst and produce a more rigorous predictive model for the FBR. On the other hand, very little attention was paid in the previous literatures to the application of steady-state simulation and process improvement for an existing industrial Unipol® polypropylene plant. Accordingly, the developed model in this work has been utilized for investigating the effect of different process variables on process performance and for process improvement.

2. Modeling Methodology

2.1 Process description

The Unipol® polypropylene plant under investigation was originally developed by Dow Company, a major worldwide licensor for polypropylene technologies (Biron, 2018). The plant was established in 2001 and has a production capacity of 120,000 metric tons per year. The fourth generation of Z-N catalysts (SHAC®) is utilized in this plant to generate different polypropylene grades such as SB-25, RF-03, RF-05 and FM-03. The key part of this industrial plant is the FBR (Fig. 1), where small catalyst (CAT or $TiCl_4$) particles (20-80 μm in diameter), suspended in white mineral oil to facilitate pumping them, are continuously fed into the FBR at a point above the gas distributor. On the other hand, triethyl aluminum cocatalyst (COCAT or TEAL) and stereospecific control agent (SCA or TAPB) are fed into the cycle gas line along with propylene monomers, recycle gases, hydrogen (chain transfer agent) and nitrogen (carrier or pressurizing agent). The CAT particles react with the incoming fluidizing monomers and other reactants, entering from the bottom, to form a broad distribution of polymer particles in the size of 100-2000 μm. After fluidization, unreacted monomers are separated in the disengagement part of the reactor. Entrained solid particles carried by the gas are segregated in the disengagement zone and are recycled back to the reaction zone. The separated gas then passes through the compressor (for fluidization) and water cooler (for exothermic heat removal) to be mixed with fresh feed and is recycled back to the reactor. The polymer product leaves the reactor from just above the distributor and is collected in a batch-wise system called a product discharge system. Normally, polypropylene production in the industrial scale through gas-phase FBRs is performed within a temperature range of 60-80 ^{o}C and a pressure range of 20-40 bar.

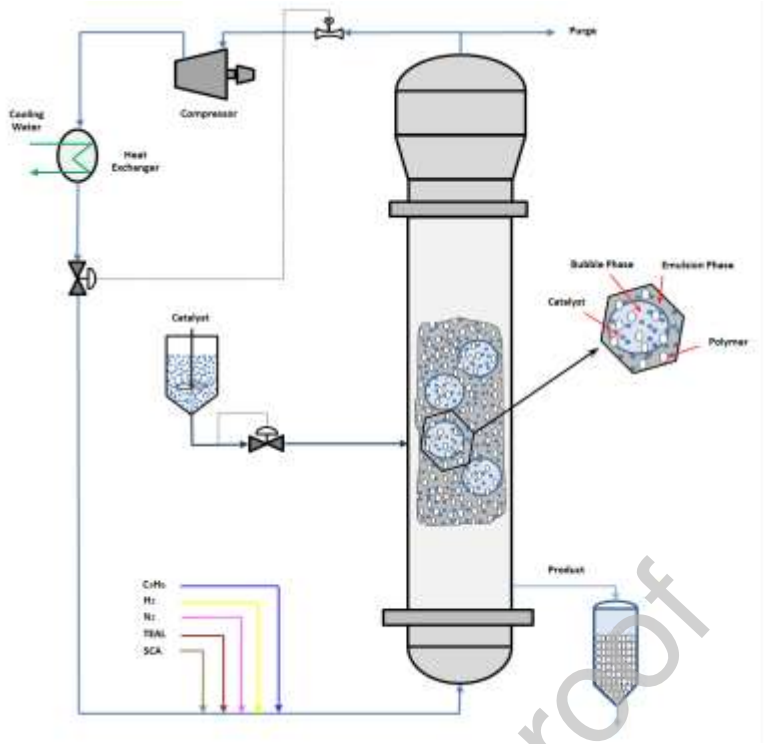

Fig. 1. An industrial Unipol® fluidized bed polypropylene reactor (Shamiri et al., 2011; Kiashemshaki et al., 2006; Abbasi et al., 2016).

2.2 Modeling Strategy

Polymers Plus® v.9 was used in simulating the gas-phase propylene homopolymerization Z-N catalytic process to create a rigorous model for an existing Unipol® FBR. Similar to other commercial process simulators, the main principles of simulation such as choosing proper thermodynamic fluid package, suitable phase equilibrium, and proper polymerization mechanism and kinetics have to be considered. However, in case of the simulation of an FBR to have realistic results, hydrodynamic considerations should also be considered. This distinguishes the current model. The hydrodynamic parameters were integrated into this model to represent the actual fluidization state of the plant FBR. In addition, the kinetic parameters of each individual reaction occurring inside the FBR were adjusted and the model was calibrated according to samples that were routinely taken during normal operation of the

industrial unit. Fig. 2 displays the modeling procedure applied in this study for developing and validating the FBR model to match with the plant FBR performance.

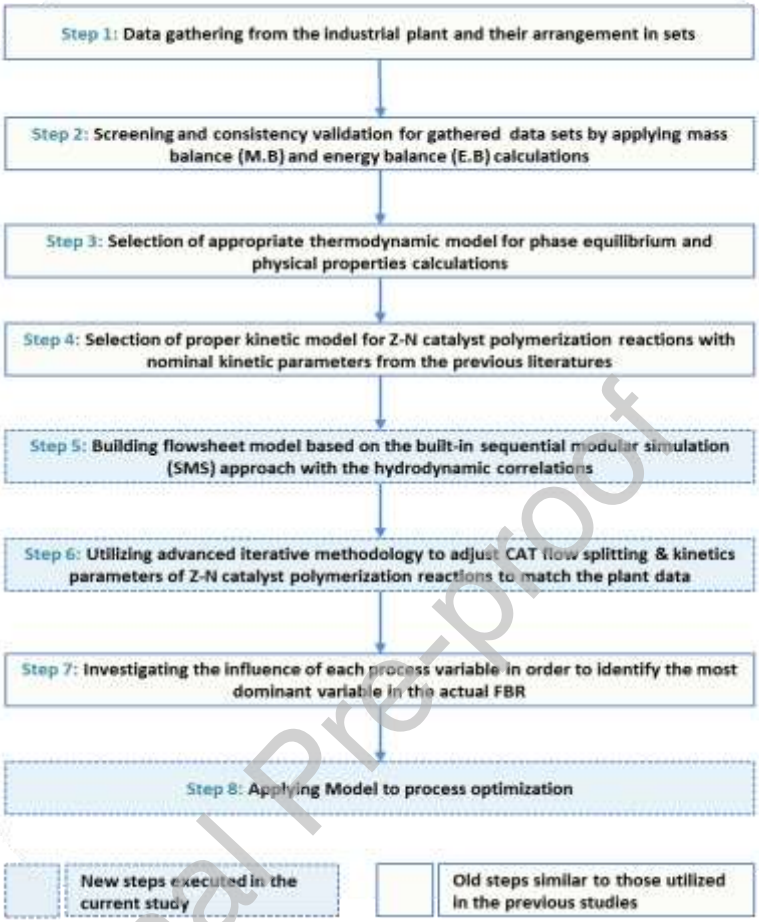

Fig. 2. Propylene polymerization process model-developing strategy.

2.2.1 Industrial Data Gathering and Arrangement

Data from the industrial homopolymerization unit under investigation were collected and arranged into data sets. Each data set represents a routine sampling for each grade of polymer produced from the plant FBR. As well, each data set includes an analysis and flow rates of all input and output streams (propylene, recycle gases, catalyst, cocatalyst, SCA, hydrogen, nitrogen and polymer) and polymer properties such as atactic ratio, melt flow, … etc. Moreover, each data set includes the operating conditions of FBR, water cooler, and recycle

gas compressor. Typically, industrial data gathered and organized into data sets were taken during steady-state operation period in order to shun erroneous results for the model.

2.2.2 Data Screening and Consistency Validation

Model quality counts mainly on the data utilized in model developing. Usually, collecting consistent data from industrial units may be challenging due to frequent fluctuations in input streams' components ratios and in process conditions. Accordingly, data sets for any of the polymer grades assembled in days that witnessed any abnormal variations in process operation were excluded. Additionally, an overall mass balance test was applied to all data sets and all data sets having a mass balance error exceeding ±2% were excluded (Sbaaei and Ahmed, 2018). For ensuring data consistency verification, a hydrogen balance was also applied to data sets by calculating the hydrogen weight in each stream and all sets having an error exceeding ±3% were excluded. (Sbaaei and Ahmed, 2018; Taskar and Riggs, 1997) Except for days that witnessed abnormal changes, most data sets were quite reliable having an average mass balance and hydrogen balance errors of -0.2306% and 0.8533%, respectively (Fig. 3).

To guarantee more precision for these data sets, an energy balance test was applied. Since the FBR under investigation operates at condensate mode, dew point calculations can represent the energy balance of the industrial FBR. Dew point calculations for gathered data sets were implemented by using Aspen Plus® user-defined correlations for components' physical properties of recycle gas stream. Thereby, the comparison between the results obtained from these calculations and the dew point analysis acquired from the industrial data sets determined which of these data should be excluded. Most data sets used in the model

building showed a quite acceptable accuracy during energy balance calculations with an average error of 1.0694% (Fig. 3).

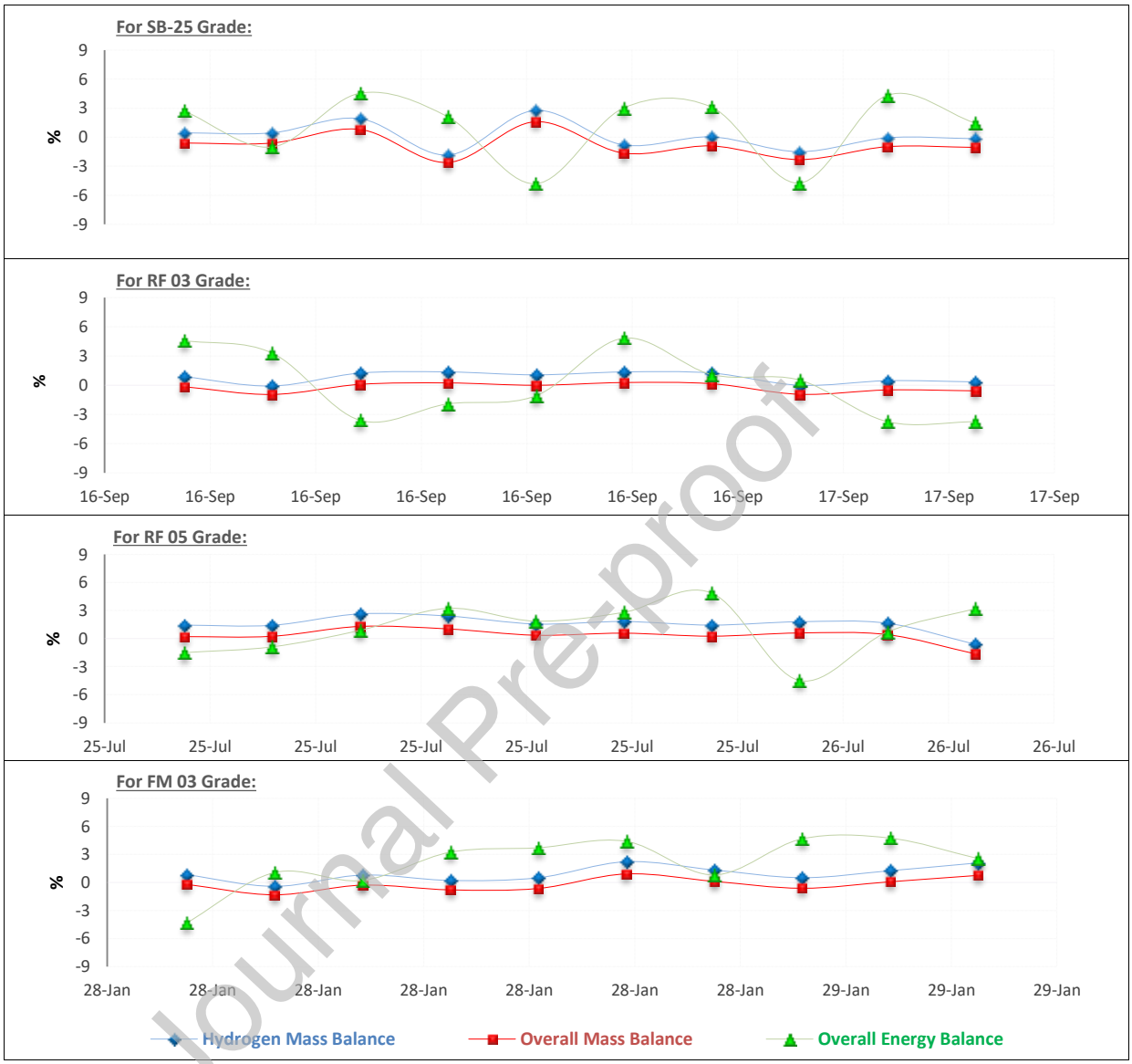

Fig. 3. Overall and hydrogen mass balance errors and overall energy balance errors for each grade of polymer.

2.3 Reactor Modeling

Polymers Plus® ships with several thermodynamic and physical models that are especially developed and extended in order to be able to deal with the polymerization systems. Among these models, the perturbed chain-statistical associating fluid theory (PC-SAFT) model suggested by Gross and Sadowski (2001) shows certain superiority (Luo et al.,

2009; Khare et al., 2004; Zheng et al., 2011). PC-SAFT model utilizes hard sphere chain principles to account for the connectivity of segments that comprise the chains, considering the interactions between these segments. Therefore, this model shows a more realistic description for the thermodynamic behavior and the phase equilibrium of mixtures with chainlike molecules while comparing its predictions with experimental data (Khare et al., 2004). In the present study, PC-SAFT model was utilized in the model development. This thermodynamic model normally requires three pure-component parameters for each pure species in the polymerization system. Thus, these parameters were taken from the reported values in the literature (Luo et al., 2009; Khare et al., 2004; Zheng et al., 2011).

On the other hand, the kinetics of propylene homopolymerization using multi-site Z-N catalysts has been extensively studied in the literature (Luo et al., 2009; Shamiri et al., 2010; 2011; 2012; Khare et al., 2004). In this model, six elementary reaction-type categories were considered commensurate with the current case. One reaction-type category may include more than one reaction as illustrated in Table 1, resulting in ten reactions at each catalyst site. Since the fourth-generation type Z-N catalyst is used in the FBR under investigation, the total reactions occurring on multiple active sites (four sites) of Z-N catalyst are up to 40 reactions. These allow the model to reach the desired properties for various polymer grades.

Table 1. Kinetic mechanism of propylene homopolymerization used in the model development.

Reaction for each catalyst site	**Description**	
1. Catalyst Activation:	$CAT_i \xrightarrow{k_{sp,i}} P_{0,i}$	(1)
	$CAT_i + COCAT \xrightarrow{k_{act,i}} P_{0,i}$	(2)
2. Chain Initiation:	$P_{0,i} + M \xrightarrow{k_{ini,i}} P_{1,i}$	(3)

3. Chain Propagation: $$P_{n,i} + M \xrightarrow{k_{p,i}} P_{n+1,i} \quad (4)$$

4. Atactic Propagation: $$P_{n,i} + M \xrightarrow{k_{pa,i}} P_{n+1,i} \quad (5)$$

5. Chain Transfer: $$P_{n,i} + H_2 \xrightarrow{k_{th,i}} D_n + P_{0,i} \quad (6)$$

$$P_{n,i} + M \xrightarrow{k_{tm,i}} D_n + P_{1,i} \quad (7)$$

$$P_{n,i} + COCAT \xrightarrow{k_{tco,i}} D_n + P_{1,i} \quad (8)$$

6. Catalyst Deactivation: $$P_{0,i} \xrightarrow{k_{ds,i}} DCAT_i$$

$$P_{n,i} \xrightarrow{k_{ds,i}} D_n + DCAT_i \quad (9)$$

$$P_{0,i} + SCA \xrightarrow{k_{dsca,i}} DCAT_i$$

$$P_{n,i} + SCA \xrightarrow{k_{dsca,i}} D_n + DCAT_i \quad (10)$$

The polymerization in the FBR is the heart of the Unipol® polypropylene plant under investigation. However, because of the negligence of hydrodynamic influences, Polymers Plus® and other similar commercial simulation programs are generally not able to deal directly with this type of reactors. These programs' library merely contains ideal reactors such as CSTR and PFR with no corresponding or appropriate module that can directly represent FBR. Many mathematical attempts in the literature were tried to find the adequate approximation for nonideal reactors and to remediate the drawbacks of their models. Nevertheless, the present model is a first attempt to create Aspen Plus® model combining thermodynamic, hydrodynamic and kinetic parameters for simulating polymerization FBRs. Lacking the hydrodynamic considerations of the FBR in the previous Aspen Plus® models impedes their applicability over a wide range of fluidization conditions. Accordingly, the current model was developed based on the SMS approach developed by Jafari et al. (2004a,b). This approach considers that the combination of the different standard modules together can indeed represent the entire process with high accuracy. Jafari et al. (2004a,b)

stated that the fluidized bed in FBRs comprises of two phases: bubble and emulsion phases. As well, this fluidized bed should be simulated as operating in its actual fluidization state, i.e. in turbulent flow regime. Therefore, they proposed that a pseudo-homogeneous isothermal CSTR is a valid hypothesis for modeling the emulsion phase of FBR whereas an adiabatic PFR is a valid assumption for modeling the bubble phase of FBR.

Three hydrodynamic parameters were integrated into the SMS approach to simulate the bubble and emulsion phases within the FBR simultaneously and to guarantee the fine-tuning for activity parameters in the following steps. The first hydrodynamic parameter, by which the model is divided into several segments in series, is to determine the number of divided segments according to the operating conditions of the plant FBR. Thus, the current two-phase FBR model was divided into four segments (Jafari et al., 2004a,b; Kiashemshaki et al., 2006; Ashrafi et al., 2012). Each segment was simulated by a CSTR for emulsion phase and a PFR for a bubble phase while the polymerization reactions considered to progress in both phases as well. The second hydrodynamic parameter was to estimate the volume fraction of each phase in each segment. Accordingly, the hydrodynamic correlations proposed by Kunii and Levenspiel (1991) and Cui et al. (2000) were applied for the current Unipol® FBR model (Table 2). The bubble phase fraction (δ_B) was calculated based on the physical properties gathered in the industrial data sets (Table 3). As a result, the volume of one CSTR was considered to equal ten times the volume occupied by its counterpart PFR (Table 4). The third hydrodynamic parameter is the ratio by which Z-N catalyst feed split in each phase. This parameter is used in evaluating the voidage inside the FBR and simulating the fluidizing phases. In this model, this parameter was considered as an adjustable parameter that can be rectified during the model development by the tuning procedure proposed in the present study.

Fig. 4 illustrates the composite Aspen Polymers® modules utilized to establish the comprehensive model representing the plant FBR. Using the SMS approach allows the model to deal with the fluidized bed of the industrial FBR operating in the turbulent flow regime, resulting in further reliability to the model outcomes. Moreover, by applying this approach, the influences of the FBR hydrodynamic parameters in the model development can be assessed, permitting to investigate and explore their effects on other operating variables. After incorporating the hydrodynamic parameters, the FBR model was integrated with the prespecified multisite kinetic scheme for Z-N catalytic polymerization (Table 1). Benefiting from Aspen Plus software package, the FBR model outcomes could be adjusted to conform to the plant FBR performance by fine-tuning the kinetic parameters of homopolymerization reactions, conducted in this work as follows.

Table 2. Hydrodynamic parameters utilized in the model development (Shamiri et al., 2011; 2012; Ibrehem et al., 2009; Kunii and Levenspiel, 1991)

Hydrodynamic Parameter	**Formula**	
Mass transfer driving force (η):	$\eta = g(\rho_c - \rho_g)$	(11)
Sphericity* (Ψ):	$\Psi = \frac{A_s}{A_p}$	(12)
	* This parameter ranges from 0.5 to 1, with 0.6 being a normal value for a typical granular solid.	
Porosity at minimum fluidization** ($\boldsymbol{\varepsilon_{mf}}$):	$\varepsilon_{mf} = 0.586 \times \Psi^{-0.72} \times (\frac{\mu^2}{\rho_g \eta d_p^3})^{0.029} \times (\frac{\rho_g}{\rho_c})^{0.021}$	(13)
	or	
	$\varepsilon_{mf}^3 = 0.091 \times (\frac{1-\varepsilon_{mf}}{\Psi^2})$	(14)
	** The value of this parameter is around 0.5.	
Minimum fluidization velocity ($\mathbf{U_{mf}}$):	$U_{mf} = \frac{\psi^2 d_p^2}{150\mu} \times \eta \times \frac{\varepsilon_{mf}^3}{1-\varepsilon_{mf}}$	(15)
Bubble phase fraction ($\boldsymbol{\delta_B}$):	For Geldart B: $\delta_B = 0.534 \times (1 - \exp(-\frac{U_0 - U_{mf}}{0.413}))$	(16)

Table 3. Physical properties used in the hydrodynamic correlations.

Physical properties	**Value**
μ (gas viscosity)	1.274×10^{-4} (Pa.s)
ρg (gas density)	68.76 (kg/m^3)
ρs (catalyst density)	2370 (kg/m^3)
dp (particle diameter)	500×10^{-6} (m)

Table 4. Calculated hydrodynamic parameters utilized in the model development.

Parameter	**Calculated value**
U_o (given)	0.354 (m/s)
Ψ (suggested by Kunii and Levenspiel (1991))	0.6
ε_{mf} (calculated)	0.524
u_{mf} (calculated)	0.271 (m/sec)
δ_B (calculated)	0.098 ~ 0.1

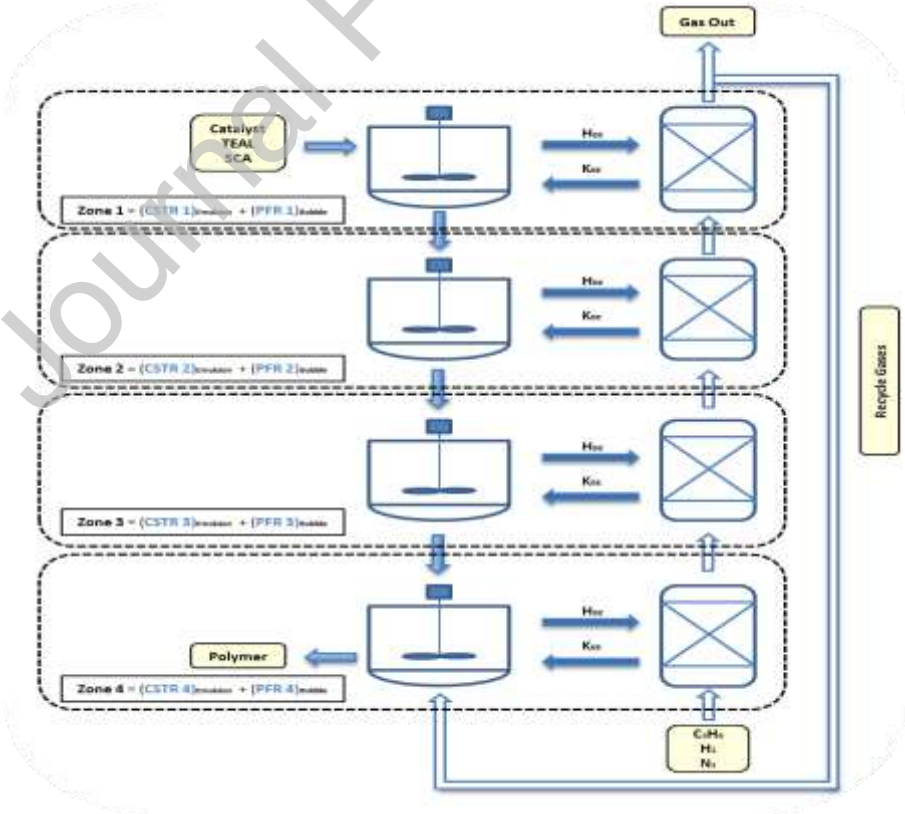

Fig. 4. Schematic diagram of the modeling structure for the two-phase FBR model.

2.4 Model Calibration and Parameters Estimation

Parameters estimation is generally the most decisive step in model development. A well-calibrated model outputs significant and repeatable prediction over a wide range of operating conditions. Awkward calibration of FBR model may lead to an over-calibrated model with a weak predictive power. In this work, the methodologies proposed by Khare et al. (2002, 2004) and Luo et al. (2009) were adopted and developed to be applicable with the current case. In addition, the advanced tuning tools provided in Aspen Plus software were used to create an advance iterative methodology that can deal with multiple data sets gathered from the industrial plant. Since the polymerization reactions are highly coupled, varying a single kinetic parameter results in several synchronized changes in the simulation variables. This makes parameters tuning more complicated and difficult. Hence, this advanced tuning allows the user to match plant performance through tuning all adjustable parameters simultaneously. Model developers allege that if the tuning of FBR model is enough to match plant data, the prediction power of this model seems to be extremely rigorous in tracking plant performance. Fig. 5 shows the two-step tuning process methodology applied in the developed model.

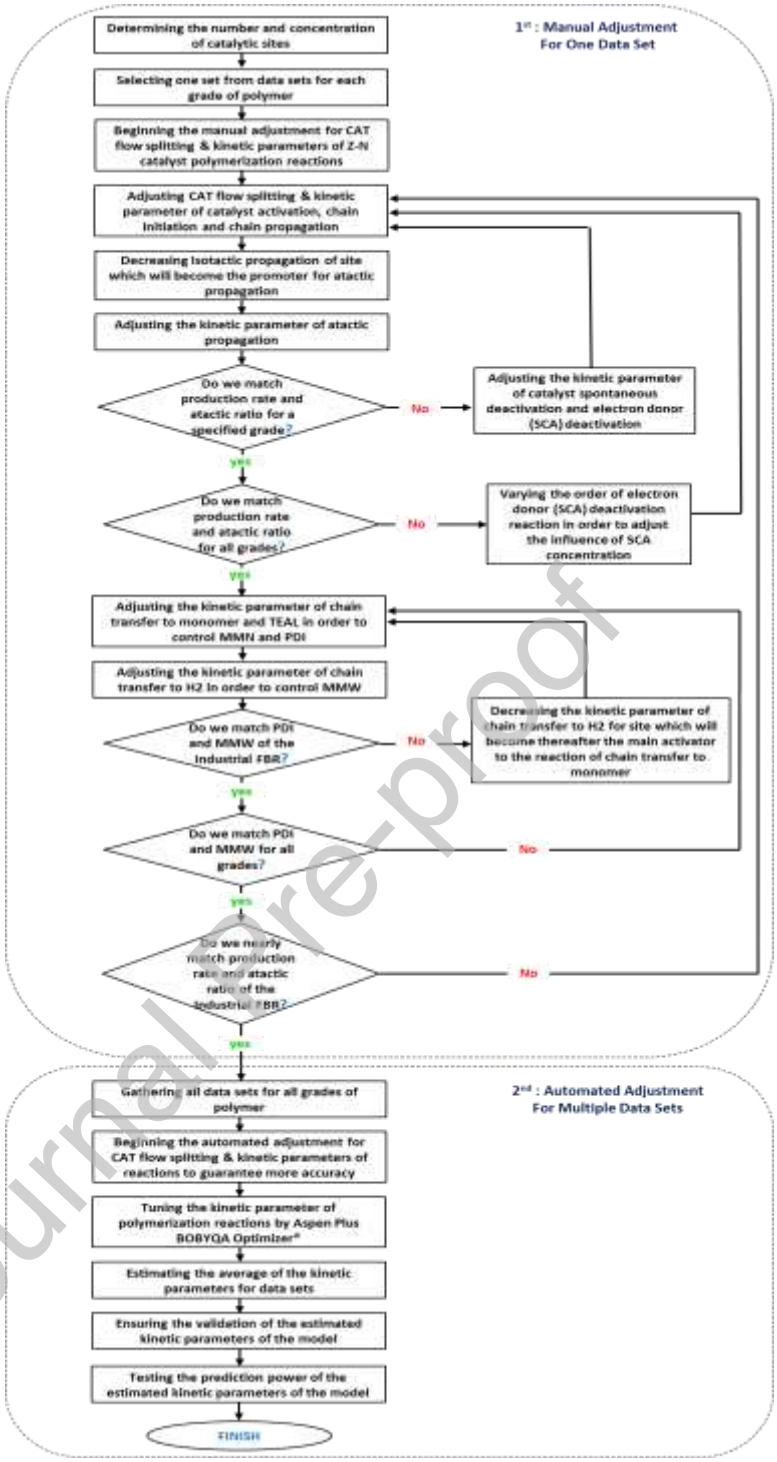

Fig. 5. Advanced Iterative methodology applied in the multisite developed model to adjust the kinetic parameters.

Utilizing the two-step tuning process methodology for setting a multiset of kinetic parameters allows the model to accurately predict the properties of several polymer grades. In the first step, one data set from the plant is manually adjusted according to the assumptions

suggested by Khare et al. (2002, 2004). The initial values of the kinetic parameters, at which the first step of tuning process begins, can be estimated through Gel Permeation Chromatography (GPC) distribution data. The objective of this step is to reach rough values for adjustable parameters to be usable in the second step. To improve the reliability of these parameters, the second step should be adopted. In this step, an automated iterative adjusting for adjustable parameters by Aspen Plus® tools is used for multiple data sets. The iterations are completed when these parameters allow the model to match all simulation targets for all polymer grades. For rigorous representation of the plant FBR, the next steps were pursued:

2.4.1 Running the model

Each data set was used to produce streams for each compound introduced into the FBR and to generate a recycle gas stream at the operating day that each data set represents. The reactor model requires some mechanical data such as reactor dimensions and its fluidized bed volume. In addition to these data, the operating conditions and holdup specifications should be specified. As mentioned before, the correlations provided by Kunii and Levenspiel (1991) and Cui et al. (2000) were used to estimate the volume of the FBR fluidizing phases.

For the purpose of speeding flowsheet convergence, Aspen Plus Calculator® was utilized in the model development. Since a recycle stream exists in this model, FORTRAN statements were incorporated into Aspen Plus Calculator® in order to feed-forwardly control input variables. This technique decreases the number of iterations required to convergence the model simulation. Otherwise, the kinetics of polymerization reactions exhibit very difficult convergence troubleshoots. Consequently, the standard convergence options are often deficient and inept. Therefore, Newton method was utilized to control the convergence of the calculations in this model. In addition, Line Search method was used as a stabilization strategy for stabilizing the Newton algorithm. This method, which is recommended for polymerization reactions, utilizes one dimensional search along Newton direction. The

component-based scaling was also used to scale each variable independently. This scaling leads to tight tolerances and more accuracy. After identifying these specifications, the FBR model was allowed to run generating output streams. On the other hand, other equipment existing with the FBR such as water cooler and recycle gas compressor were readily simulated by information provided from the data sets of the industrial plant.

2.4.2 Model calibration

Reactor model calibration is a two-step adjustment process for adjustable parameters in order to match plant data. In this work, the FBR model was calibrated with the aid of an advanced iterative methodology adopted by Aspen Plus BOBYQA (Bound Optimization By Quadratic Approximation) Optimizer® by applying the least squares (LS) principle to minimize the following objective function:

$$f(x) = \sum_{j=1}^{n} (w_j \times (X_{model,j} - X_{plant,j})^2) \quad (17)$$

The activity parameters of polymerization reactions and the catalyst flow splitting in each phase of the fluidized bed were manually tuned by the first tuning-step to determine the bounds of the parameters change. Then, the adjustable parameters were automatically tuned by the advanced iterative BOBYQA technique to minimize the gap between the model outcomes and the plant data for multiple data sets. These parameters were normalized in the second tuning-step by specified lower and upper bounds without exceeding the range between them in order to avoid numerical problems during the model calibration.

It is imperative not to comprise all measurements of an industrial plant Unipol® FBR in reactor model calibration. Pashikanti and Liu (2011) have used advanced software simulators for modeling industrial units and they cautioned that including all measurements in reactor model calibration may yield to a weak calibrated model that responds violently,

even to any slight change in operating variables. Polypropylene production rate (PPR), melt flow index (MFI), atactic fraction (ATFRAC), and polydispersity index (PDI) (simulation targets) were the measurements of the plant FBR used in this model. The MFI of the polymer grades was used as an indicator to the changes in MWW of the product generated from the plant FBR. Therefore, the equation of MFI proposed by Pasquini (2005) for the bulk polypropylene was utilized in this study. Routine sampling from the industrial unit under investigation was carefully taken while calibrating the kinetic parameters to match a specific production line and product grade. Therefore, PPR, MWW, ATFRAC and PDI were included as process variables in the optimization function for the model calibration.

Weighting factors were exploited to provide more significance to certain variable in a group of variables. Moreover, these factors could be utilized to regulate the difference in variables measurement units. For example, production rate is measured in kg/h, MWW in kg/mol and ATFRAC in molar percentage, whereas PDI is dimensionless. On the other hand, large weighting factors were applied for terms where a closer fit is mandatory. On the contrary, lowest weighting factors were applied for less important terms. Although most terms have the same degree of significance, weighting factors were applied in this model for adjusting the variables measurement units. Table 5 shows the FBR measurements that were included in optimization function and weighting factors used with them.

Table 5. Terms included in objective function for reactor model calibration and applied weighing factors.

Term	Applied Weighting Factor
PPR [kg/h]	1
MWW [kg/mol]	10
PDI	1000
ATFRAC [mol.%]	1000

The three preceding steps were repeated for each data set and adjustable parameters were calculated separately for each. Roughly all adjustable parameters for different data sets were found to vary within a constricted range. Thus, the average values of calculated parameters are anticipated to be extremely acceptable for the model calibration. Table 6 and 7 show the average of adjustable parameters estimated through the calibration process for the FBR.

Table 6. Estimated average activity parameters for multisite Z-N catalyst.

Rxn-Type	**Site No.**	**Comp 1**	**Comp 2**	**Average Pre-Exp**	**Act-Energy***	**Order***	**Ref. Temp. (T_{ref})**
Unit				1/sec	J/kmol		K
ACT-SPON	1	CAT		0.000165	31987152	1	333
ACT-SPON	2	CAT		0.000210	31987152	1	333
ACT-SPON	3	CAT		0.000134	31987152	1	333
ACT-SPON	4	CAT		0.000138	31987152	1	333
ACT-COCAT	1	CAT	TEAL	0.000006	31987152	1	333
ACT-COCAT	2	CAT	TEAL	0.000007	31987152	1	333
ACT-COCAT	3	CAT	TEAL	0.000005	31987152	1	333
ACT-COCAT	4	CAT	TEAL	0.000005	31987152	1	333
CHAIN-INI	1	C3H6		101.9689	30144960	1	333
CHAIN-INI	2	C3H6		43.67381	30144960	1	333
CHAIN-INI	3	C3H6		105.9423	30144960	1	333
CHAIN-INI	4	C3H6		37.56962	30144960	1	333
PROPAGATION	1	C3H6-R	C3H6	138.4189	30144960	1	333
PROPAGATION	2	C3H6-R	C3H6	127.3062	30144960	1	333
PROPAGATION	3	C3H6-R	C3H6	84.18851	30144960	1	333
PROPAGATION	4	C3H6-R	C3H6	21.55753	30144960	1	333
CHAT-MON	1	C3H6-R	C3H6	0.056922	52000000	1	333
CHAT-MON	2	C3H6-R	C3H6	0.048214	52000000	1	333
CHAT-MON	3	C3H6-R	C3H6	0.000011	52000000	1	333
CHAT-MON	4	C3H6-R	C3H6	0.002052	52000000	1	333
CHAT-COCAT	1	C3H6-R	TEAL	0.585743	50241600	1	333
CHAT-COCAT	2	C3H6-R	TEAL	0.530683	50241600	1	333
CHAT-COCAT	3	C3H6-R	TEAL	0.437354	50241600	1	333
CHAT-COCAT	4	C3H6-R	TEAL	0.146309	50241600	1	333
CHAT-H2	1	C3H6-R	H2	10.21988	44798760	1	333
CHAT-H2	2	C3H6-R	H2	0.000046	44798760	1	333

CHAT-H2	3	C3H6-R	H2	4.425521	44798760	1	333
CHAT-H2	4	C3H6-R	H2	0.000038	44798760	1	333
DEACT-SPON	1			0.000095	4186800	1	333
DEACT-SPON	2			0.000096	4186800	1	333
DEACT-SPON	3			0.000095	4186800	1	333
DEACT-SPON	4			0.000001	4186800	1	333
ATACT-PROP	1	C3H6-R	C3H6	0.009852	30144960	1	333
ATACT-PROP	2	C3H6-R	C3H6	0.021154	30144960	1	333
ATACT-PROP	3	C3H6-R	C3H6	0.245973	30144960	1	333
ATACT-PROP	4	C3H6-R	C3H6	34.69585	30144960	1	333
DEACT-EDONOR	1	TAPB		0.085743	4186800	1	333
DEACT-EDONOR	2	TAPB		0.739684	4186800	1	333
DEACT-EDONOR	3	TAPB		0.071781	4186800	1	333
DEACT-EDONOR	4	TAPB		1.787719	4186800	1	333

* These values used in the rate equation of each elementary reaction were obtained from the literature (Luo et al., 2009; Khare et al., 2004; Zheng et al., 2011)

Table 7. Estimated average of split of catalyst flow rate in each phase of the fluidized bed.

Term	**Bubble phase**	**Emulsion phase**
CAT flow fraction	0.34	0.66

Fig. 6 shows the model performance versus the plant yields for the 40 data sets (10 sets for each polymer grade) used in the calibration process. This parity plot shows that the model predictions match with the plant data in an excellent way. It should be clarified here that a closer fit might be achieved with increasing the number of evaluations utilized and the number of variables involved in the optimization function. This requires quite numerous measurements of the industrial plant, which were unavailable. However, a closer fit during the calibration may result in creating a model with poor-predictive capabilities over a wide range of input variables (Sbaaei and Ahmed, 2018; Pashikanti and Liu, 2011).

In this study, the FBR model was simulated as four reaction zones each consisting of an adiabatic PFR for the bubble phase and an isothermal CSTR for the emulsion phase (SMS

approach). Thus, the thermal profile of the model differed from that of the actual FBR. Therefore, after completing the tuning of the kinetic parameters, the thermal profile along the plant FBR should be simulated. Theoretically, the temperature distribution of the FBR can be mainly represented by simulating the thermal profile for the emulsion phase because most of the fluidized bed volume is occupied by the emulsion phase under the operating conditions of industrial FBRs (estimated at 90% of the FBR in the current case). Since the simulated four reaction zones are not actually separated from each other, the heat transfer between them cannot be neglected. Therefore, the tuned kinetic parameters and the actual FBR temperatures from the industrial data sets were utilized to estimate the thermal profile of the FBR model.

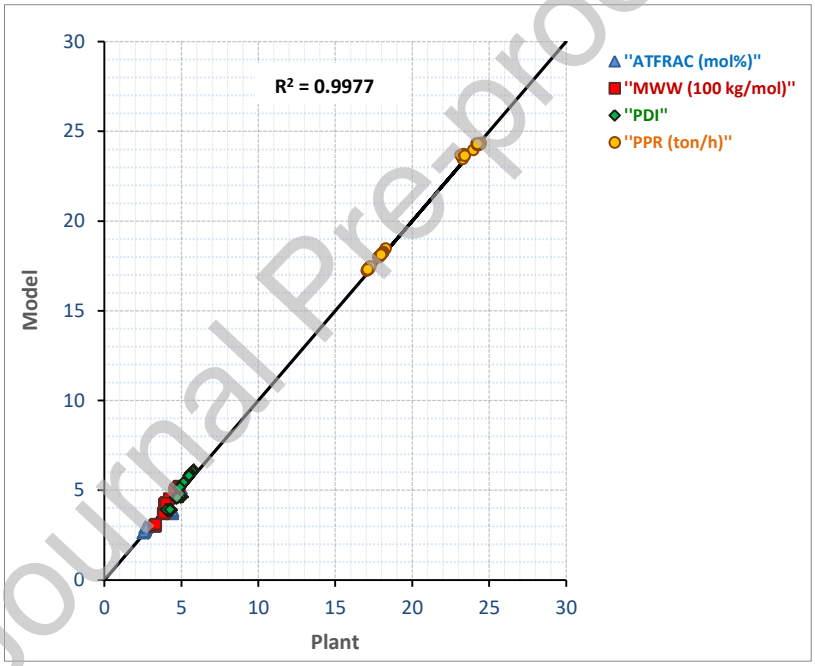

Fig. 6. Plant versus model with model calibration data sets for all polymer grades.

2.5 Model Testing and Validation

To ensure the model prediction power, the yields of this fine-tuned model were compared with the yields of the plant FBR for each polymer grade as well as their specifications within period ranging from 1 to 4 months after the calibration period. As such, the model validation was implemented with new 40 data sets (10 sets for each polymer

grade). The data sets utilized in the validation test include: the FBR production rate (PPR) and the polymer properties such as MWW represented by the MFI, degree of crystallinity represent by ATFRAC, and MWN represented by PDI. The recalibration of the FBR model was not required in this step. Practically, the propylene feed of the unit under investigation is purified before introducing to the industrial FBR. Consequently, during the post-calibration period, the change in the catalyst activity was neglected in the developed model because of the absence of the impurities. Fig. 7 shows an excellent fitting between the model outcomes and plant FBR yields with high coefficient of determination. Obviously, the model is quite successful in tracking the plant performance during post-calibration periods.

The represented calculations exhibited here demonstrate the power of this developed model, showing a predictive simulation for the plant performance at different operation conditions. Consequently, several operational endeavors such as a monitoring possibility for the catalyst activity, an accurate investigation for the operating variables and a reliable optimization for the process to fulfill the minimal operating costs can be executed in the current study. By the present modeling technique, the model allows the user to study the influence of superficial gas velocity (SGV) which Shamiria et al. (2012) failed to study its influences via Aspen Plus software, and thus optimizing industrial FBRs.

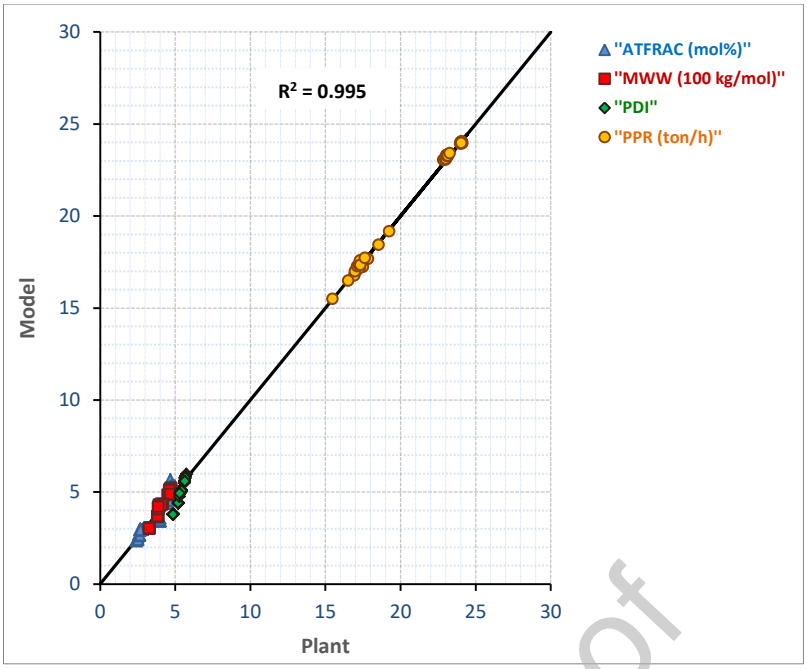

Fig.7. Plant versus model during extended periods after the calibration.

3. Results and Discussion

3.1 Process Variables

Having established a process model for Unipol® FBR, the following step is to investigate the effects of each process variable in order to predict the process performance with operating variable change. Analyzing the effect of each process variable is compulsory for process optimization. The subsequent study was implemented using the average composition of the industrial unit feed during the study period for producing a specified polymer grade (SB-25). In addition, each variable was investigated individually whereas the rest of the variables were constant. Table 8 represents the basic process variables of the FBR under investigation for generating the polymer grade SB-25.

Table 8. Basic process variables of the FBR for producing grade SB-25.

Process Variable	Unit	Value
Catalyst mass flow	kg/h	0.7
TEAL mass flow	kg/h	2.57
SCA mass flow	kg/h	1.79
Recycle mass flow	tonne/h	815
%C3=	wt.%	84.104
%C3	wt.%	10.281
%H2	wt.%	0.086
%N2	wt.%	5.529
Pressure	bar	34
Reactor Bed Temperature	^{0}C	74

3.1.1 Catalyst

Naturally, the fourth generation Z-N catalysts composed of $TiCl_4$ supported on $MgCl_2$ contains approximately 2.8 wt.% titanium and a phthalate based internal donor. Titanium, transition metal, which is the center of the catalyst molecule, has a valence state ranging from +2 to +4. However, the valence state of three (Ti +3) shows no activity towards the propylene polymerization (Skoumal, 2007; Soga and Shiono, 1997; Dehghani, 2012). The empty orbital provided by titanium atom is the active site of catalyst required for the polymerization. Typically, $MgCl_2$ supported-titanium Z-N catalysts consist of multiple active sites and each site can motivate the polymerization reactions including activation, initiation, chain propagation, chain transfer and deactivation reactions.

The molar flow rate of potential active sites into the FBR is ascribed to the mass flow rate of the catalyst. The latter is evaluated as a substantial parameter in the operation of industrial FBRs. This is reflected in Fig. 8 (A-D) that shows the catalyst effect on the FBR productivity and the polymer properties. The production rate increases with the catalyst flow due to the increase in the available active sites which boost the chain propagation (Fig. 8A).

On one hand, the increase of active sites allows the distribution of monomers on more growing chains and hence a lower MWW and MWN of the polymer (Figs. 8B and 8C, respectively). On the other hand, because of higher concentrations of other aspecific sites introduced into the polymerization system, an increase in the catalyst flow rate increases the atactic ratio in the polymer (Fig. 8D), thus the degree of the product crystallinity decreases.

The variation of catalyst feed rate strongly affects the temperature distribution through the FBR bed (Fig. 9). Accordingly, the production rate in this system is limited by heat removal from the circulating gas. To sustain satisfactory production rate, it is compulsory to hold the bed temperature above the dew point of the reactants to avert gas condensation and below the melting point of produced polymer to prevent particle melting, agglomeration and thus the emergent shut-down for the FBR.

Chain-growth polymerization reactions are highly exothermic. Thus, thermal runaway may occur inside FBR during normal operation when temperature rise is out of control. At normal operating temperatures, chain-growth polymerization reactions are irreversible. In addition, no equilibrium reactions appear in this polymerization system, unlike that appears in step-growth polymerization. High FBR temperatures are favored during polymerization for increasing the velocity of reactions. However, further increase in temperature peaks results in a decrease in the Z-N catalysts activity (Skoumal, 2007; Dehghani, 2012). Once the temperature inside the industrial FBR reaches 100 ^{o}C, these catalysts are immediately dead. Thus, the Z-N catalysts exhibit self-extinguishing characteristics. Since subjecting these catalysts to high temperatures spontaneously leads to the loss in their activity, they can minimize and often eliminate the potential for sheeting or agglomerate formation under the effect of thermal runaway. This is a particularly attractive feature for the continuity of FBR operation.

Fig. 10 exhibits the variation profile of the propylene conversion with the catalyst flow rate through the two phases of the FBR fluidized bed. It is noted that a substantial quantity of polymer produced in the bubble phase and cannot be ignored, especially at higher catalyst flow rates. Comparing to the mathematic two-phase FBR model executed by Shamiri et al. (2010) at operating conditions similar to our case, there is an agreement between both models in the ratio of polymer produced in the bubble phase of the fluidized bed (roughly 9 %). The catalyst effect on the overall conversion above 0.7 kg/h becomes slightly lower compared to its influence below this flow rate (Figs. 10 and 11). Obviously, under the catalyst effect, the thermal rise causes an increase in the rate of spontaneous deactivation reaction which results in a change in the propylene conversion trend at higher catalyst flow rates.

The chemical kinetics of Z-N catalysts is characterized by a short induction time for polymerization reactions. Thus, the bulk of the polymer is produced within the first and second zones of FBR (Fig. 11A). Note also that the variation in the propylene conversion with the catalyst flow in the first zone differs from that in other zones. This observation is due to the systematic variation in the thermal rise through each zone (Fig. 11B). Normally, the influence of this thermal escalation augments the activity of catalyst deactivation reactions. Thus, the deactivation reactions boosted by the rise in the FBR temperatures compete with the chain propagation reactions promoted by the increase in the catalyst flow rate on the available active sites. Since, the thermal rise in the first zone of FBR is higher than the other zones (Fig. 11B). The deactivation reactions appear a significant effect on the trend of the propylene conversion with the catalyst flow in the first zone compared to the others.

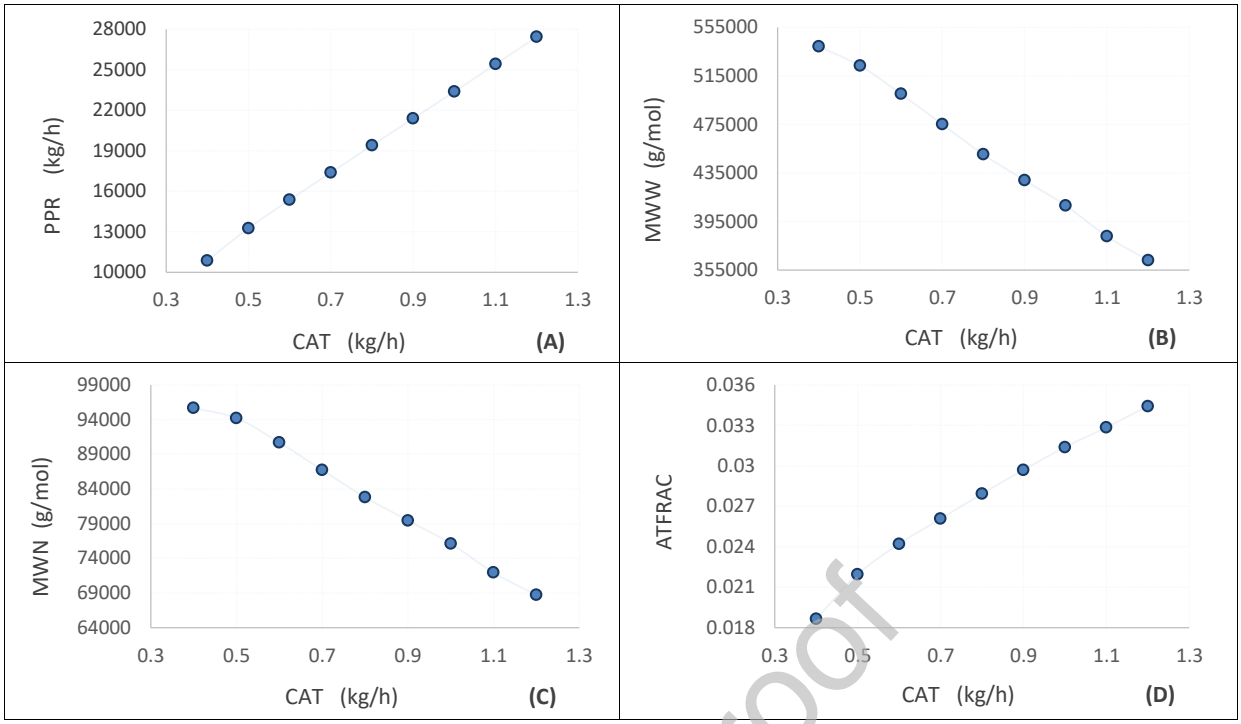

Fig. 8. Effect of catalyst flow rate on: **A**-polypropylene production rate; **B**-polymer weight average molecular weight; **C**-polymer number average molecular weight; **D**-polymer atactic fraction.

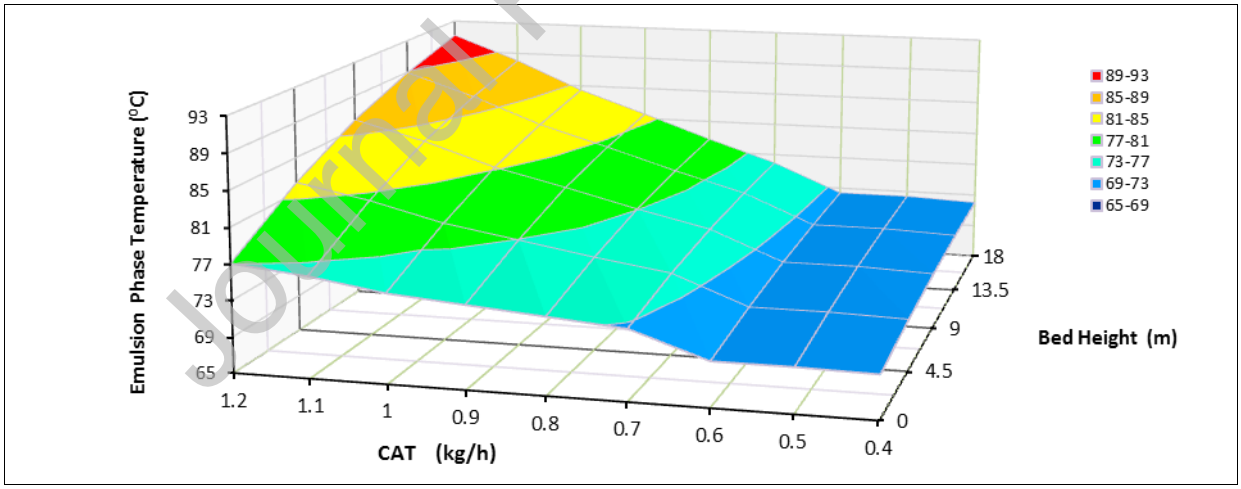

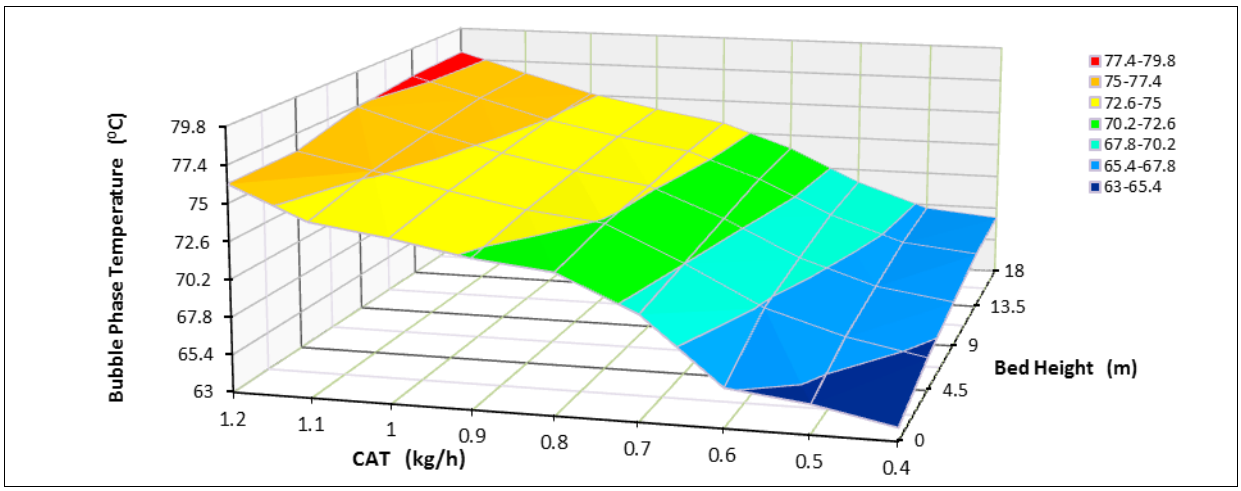

Fig. 9. Variation of FBR temperatures through the fluidized bed with catalyst flow rate.

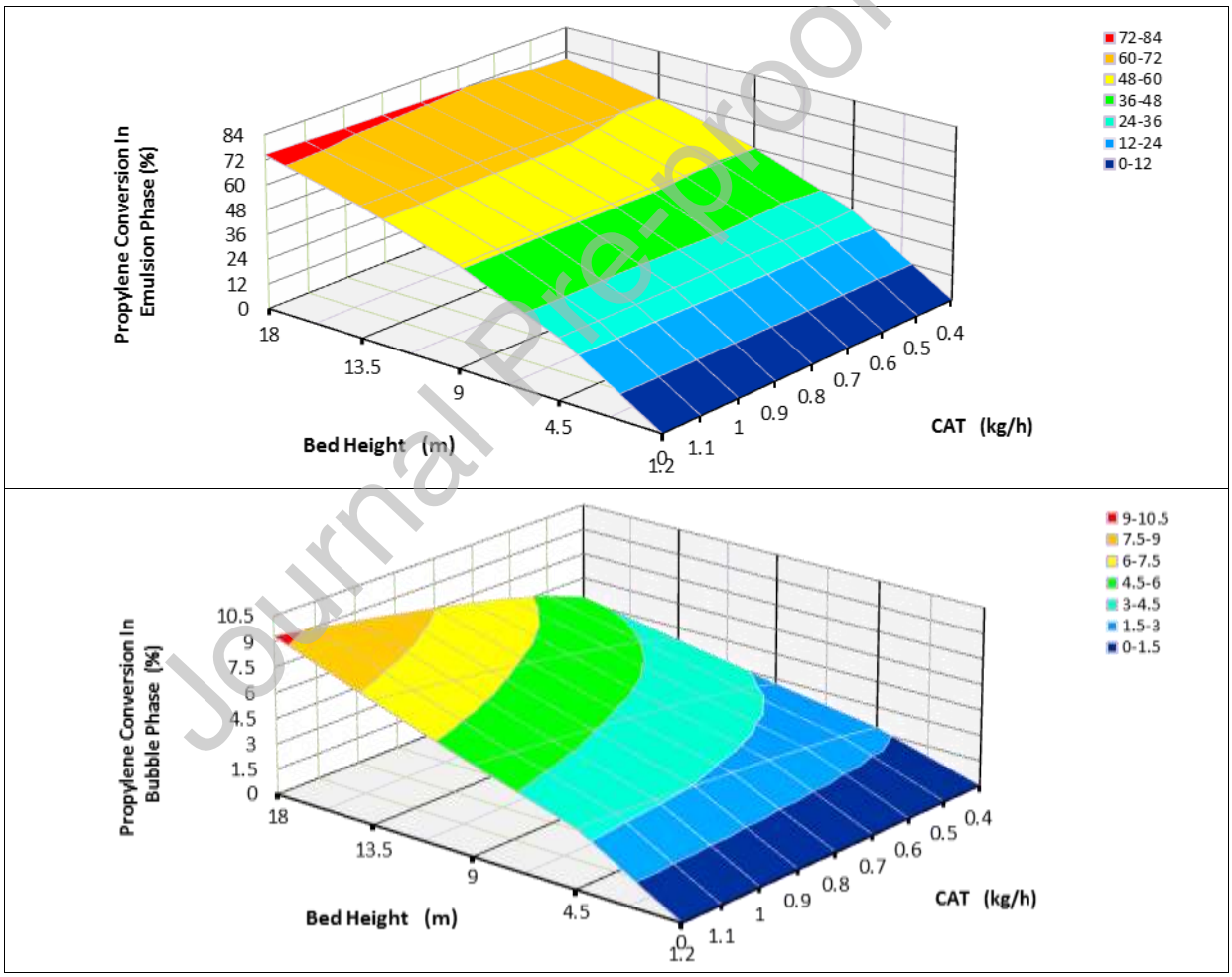

Fig. 10. Variation of propylene conversion through the fluidized bed with catalyst flow rate.

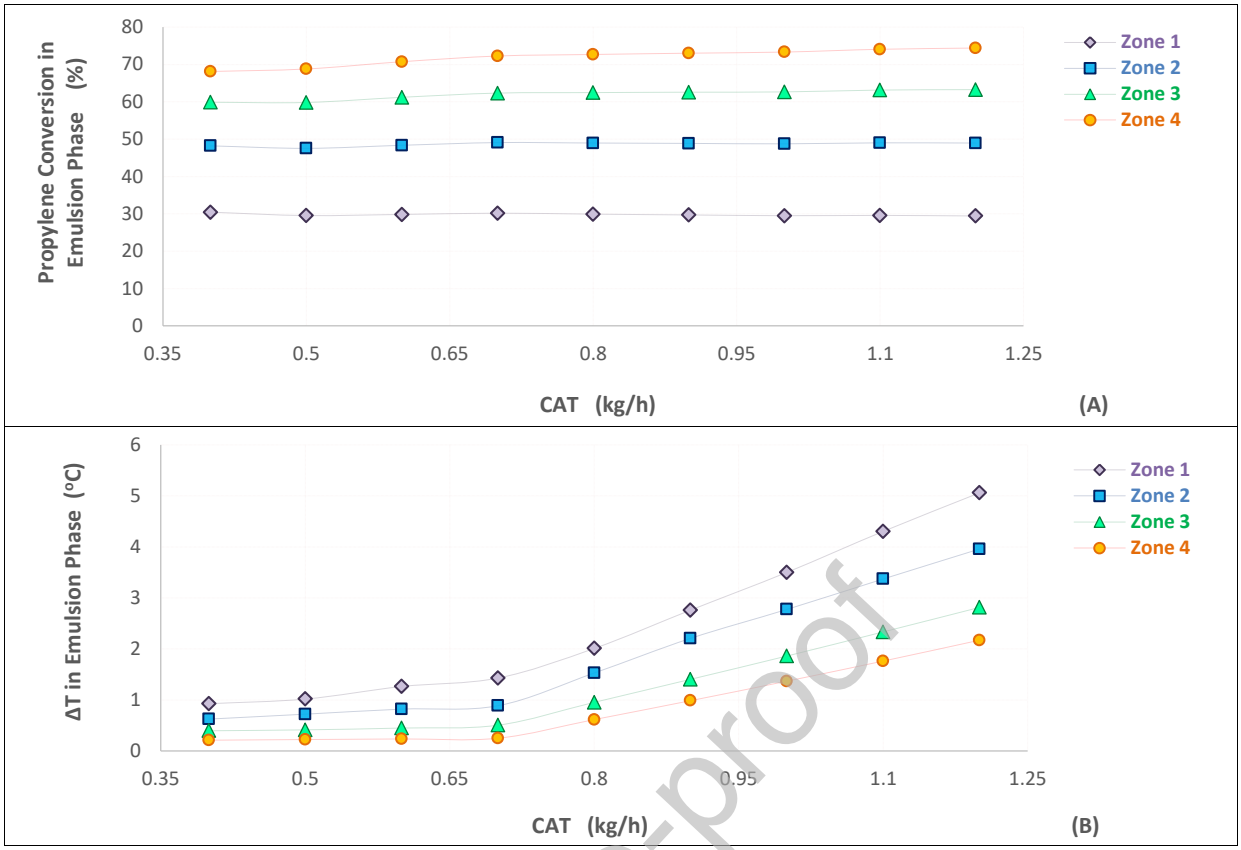

Fig. 11. Effect of catalyst flow rate on: **A**-propylene conversion through each zone of the emulsion phase; **B**-thermal rise through each zone of the emulsion phase.

3.1.2 Stereospecific Control Agent

SCA is an external electron donor that provides two functions inside the polymerization system. The first function is to deactivate the catalyst sites that promote the atactic propagation, whereas the second is to block the vacant sites on the $MgCl_2$ surface to stabilize the active sites. However, the execution of the second role is closely relevant to an internal electron donor already present in the original catalyst (Skoumal, 2007; Dehghani, 2012). SCA is supposed to control the polymer stereospecificity, either through selective poisoning for the atactic propagation active sites or through changing these aspecific sites into isospecific ones. The use of SCA in the polymerization system may also lead to the formation of new isoapecific active sites.

SCA has a considerable effect inside FBR, completely opposite to the catalyst influence. This is reflected in Fig. 12(A-D) that represents the SCA effect on the FBR productivity and the polymer properties. As the SCA flow rate increases, the FBR productivity and the polymer atactic ratio decrease while the polymer molecular weights (MWW and MWN) increase. The spectacle observed in Fig. 12(A-D), especially below SCA flow rate of 2.5 kg/h, is due to the variation in the thermal rise (Δt) through the FBR bed with the SCA flow shown in Figs. 13 and 14. A dramatic rise in the FBR temperatures appearing below SCA flow rate of 2.5 kg/h results in an increase in the activity of catalyst deactivation reactions. Thus, the chain propagation reactions boosted by the decrease in the SCA flow rate compete with the deactivation reactions promoted by the rise in the FBR temperatures on the available active sites. Since the thermal rise in the first zone of FBR is often higher than the other zones (Fig. 14B), the SCA effect (or even catalyst as stated earlier) on the propylene conversion in the first zone of the FBR becomes lower than other zones (Fig. 14A), or more scrupulously, its effect is almost intangible. However, it should be noted here that the SCA whole effect on the overall propylene conversion overcomes the thermal rise influence at the end of competition, exactly as happened with the catalyst (Figs. 8A and 12A).

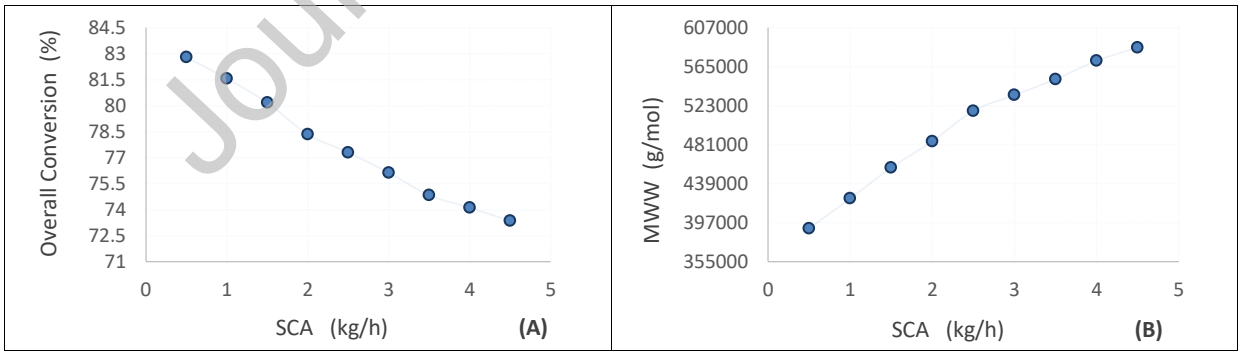

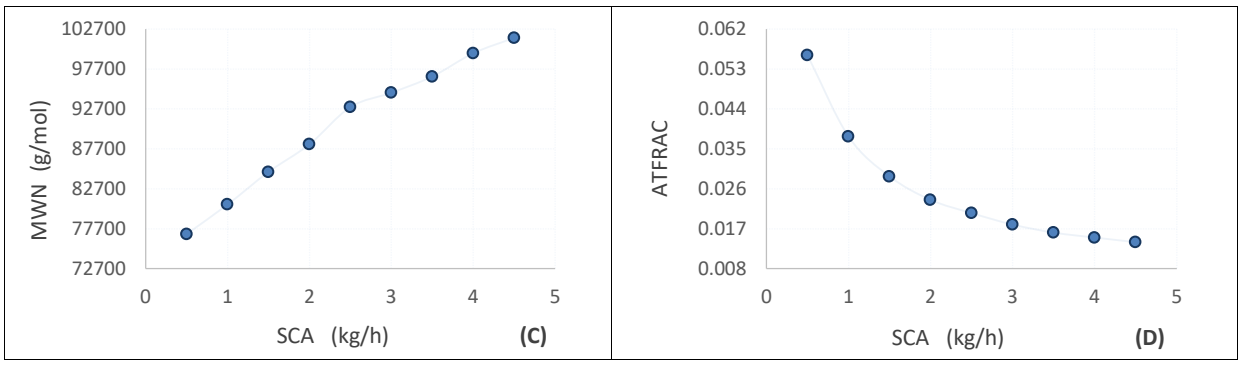

Fig. 12. Effect of SCA flow rate on: **A**-overall propylene conversion; **B**-polymer weight average molecular weight; **C**-polymer number average molecular weight; **D**-polymer atactic fraction.

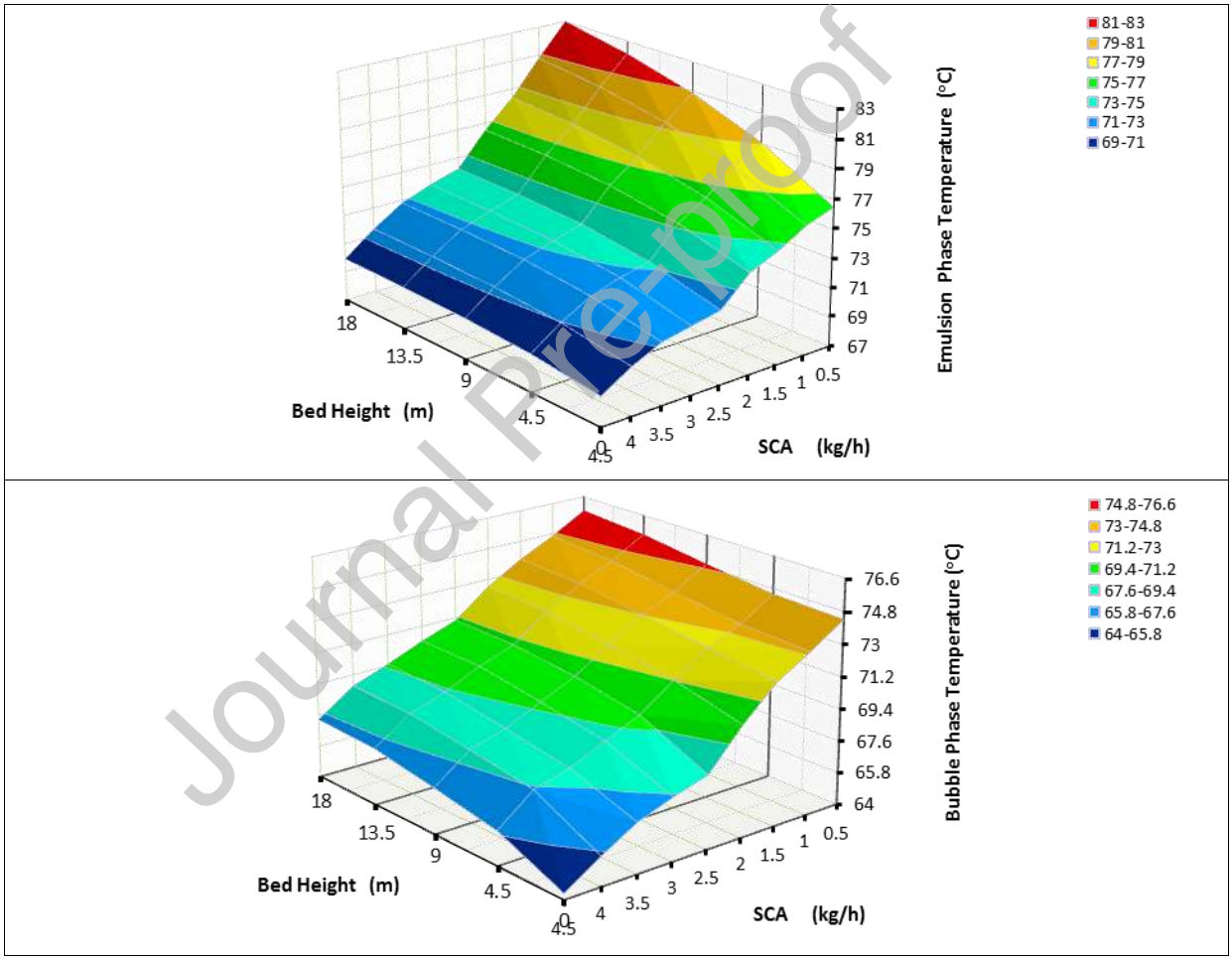

Fig.13. Variation of FBR temperatures through the fluidized bed with SCA flow rate.

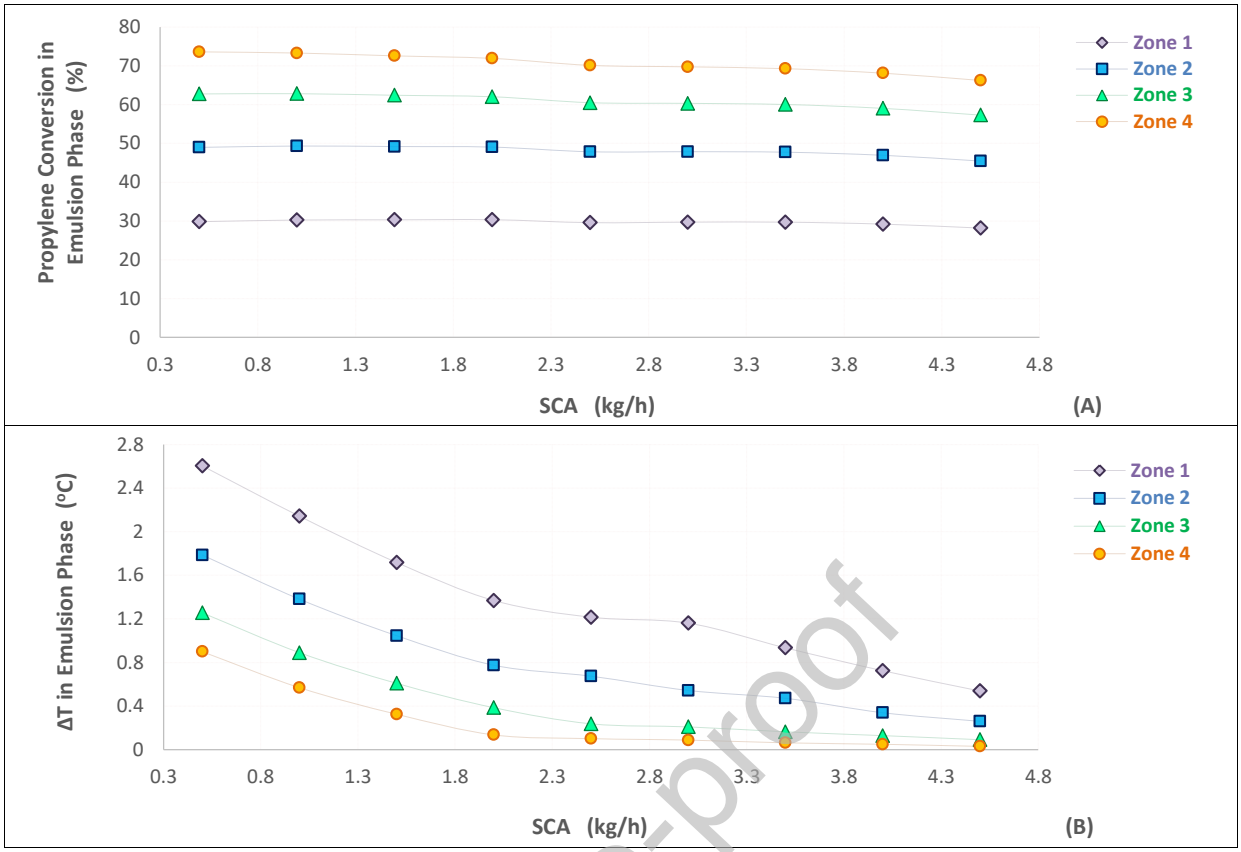

Fig. 14. Effect of SCA flow rate on: **A**-propylene conversion through each zone of the emulsion phase; **B-** thermal rise through each zone of the emulsion phase.

3.1.3 Superficial Gas Velocity

Superficial gas velocity (SGV) is a significant parameter in the operation of industrial FBRs. Not only this parameter directly controls the residence time of monomers inside these reactors, but also it provides enough heat sink to absorb continuously the heat of polymerization reactions. Thus, this hydrodynamic parameter, SGV, has a dominant effect on other process variables and directly relates to the reactor temperature. Generally, increasing SGV leads to faster movement for gases through the bed and lower mean residence time inside FBRs. Some monomers may bypass the catalyst. As well, the thermal profile of the FBR falls under the heat removal influence of SGV. Thus, the activity extent of all reactions in the polymerization system are reduced. Fig. 15 illustrates that the increase in the SGV inside the FBR results in a higher convective cooling capacity of gases passing through the

fluidized bed, leading to a lower temperature inside the reactor and vice versa. Therefore, the rate of chain propagation reaction decreases inside the FBR at higher SGVs, reducing the monomer conversion and the polymer production rate (Fig. 16 and 17A, respectively). In addition, the rate of chain transfer to hydrogen and monomer slow down, leading to higher polymer molecular weights (MWW and MWN) as exhibited in Fig. 17B and 17C, respectively. On the other hand, a decrease in FBR temperatures triggered by higher SGVs retards the rate of catalyst deactivation by SCA and atactic propagation. However, the temperature effect on the first reaction is stronger, causing the increase in atactic ratio of the produced polymer (Fig.17D), overcoming the direct effect of temperature drop on the atactic propagation.

According to Fig. 15, it can be observed that the temperature distribution is uneven at low SGVs. Meanwhile, when the velocity inside the FBR exceeded 0.44 m/sec (recycle rate of 10 ton/h), the temperature distribution becomes uniform and the rate of all polymerization reactions becomes approximately constant. Therefore, at higher SGVs, the performance of the FBR model approaches the CSTR model. This means that the fluidization regime of the fluidized bed of the plant FBR transfers from the turbulent regime (as in our case) to the fast fluidization regime at higher SGVs. This emphasizes that in our case, the well-mixed hypothesis considered by previous Aspen Plus® model developers (Luo et al., 2009) may become close to reality only when SVG inside the FBR exceeds 0.44 m/sec. Practically, the optimal SGV inside Unipol® FBRs depends mainly on reaction kinetics, FBR volume, safe operation mode, as well as economic criteria involving the power consumption of gas compressor and the utility consumption of water cooler. It is observed in Fig. 15 that the minimum temperature distribution through the FBR occurs near 0.354 m/sec (recycle rate of 8 ton/h). This observed drop in temperature distribution happens because the maximum polytropic efficiency of the recycle gas compressor is at 0.354 m/sec, resulting in lower

power and utility consumption required for the FBR cycle. It is also observed that the safe limit of operation (80 ^{o}C) will be exceeded if the recycle gases flow rate becomes less than 6 ton/h (SGV of 0.27 m/sec), viz. minimum fluidization velocity (U_{mf}) of the investigated FBR, as aforementioned.

On the other hand, based on hydrodynamic mathematical correlations (Shamiri et al., 2012), the higher the recycle gases velocity than minimum fluidization, the less the volume occupied by the bubble phase, till the volume (δ_B) reaches zero and the entire fluidized bed is considered as an emulsion phase represented by a pseudo-homogeneous isothermal CSTR. Thus, the compatibility between the inferences of this model and other mathematical models (Mahecha-Botero et al., 2009; Shamiri et al., 2010; 2011; Abbasi et al., 2016) confirms the prominence of hydrodynamic parameters incorporation into the model development.

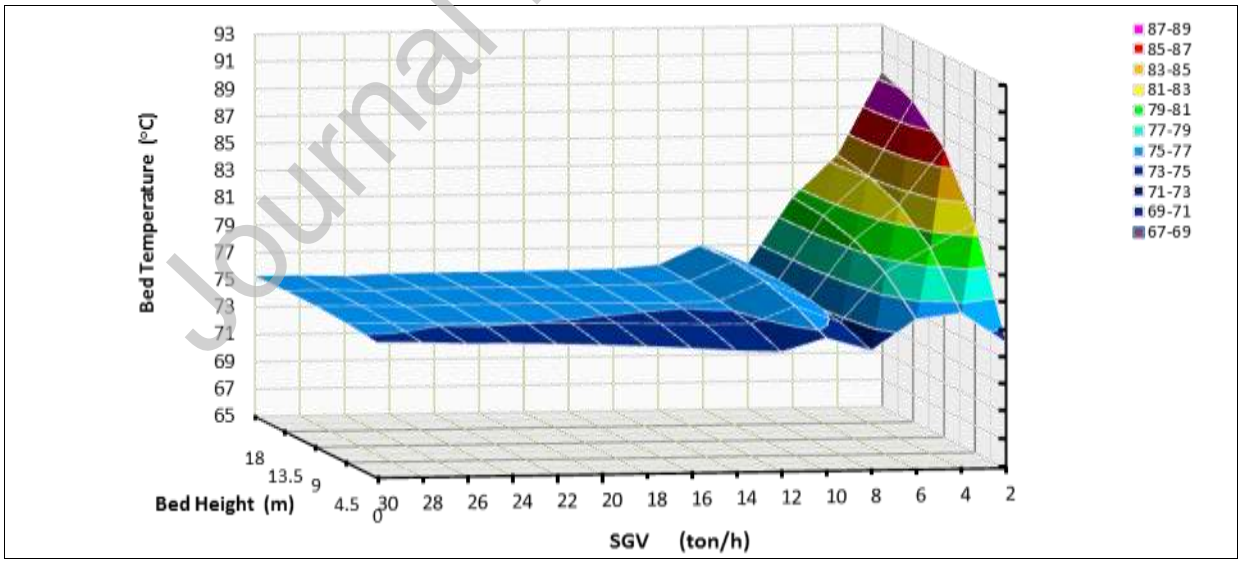

Fig.15. Variation of FBR temperatures through the fluidized bed with SGV.

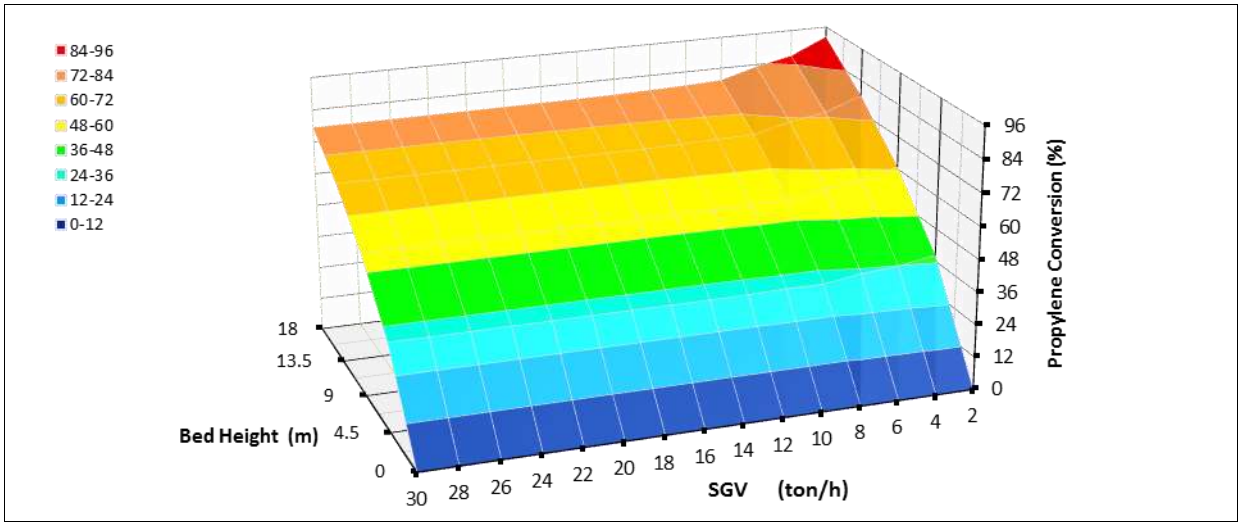

Fig.16. Variation of FBR propylene conversion through the fluidized bed with SGV.

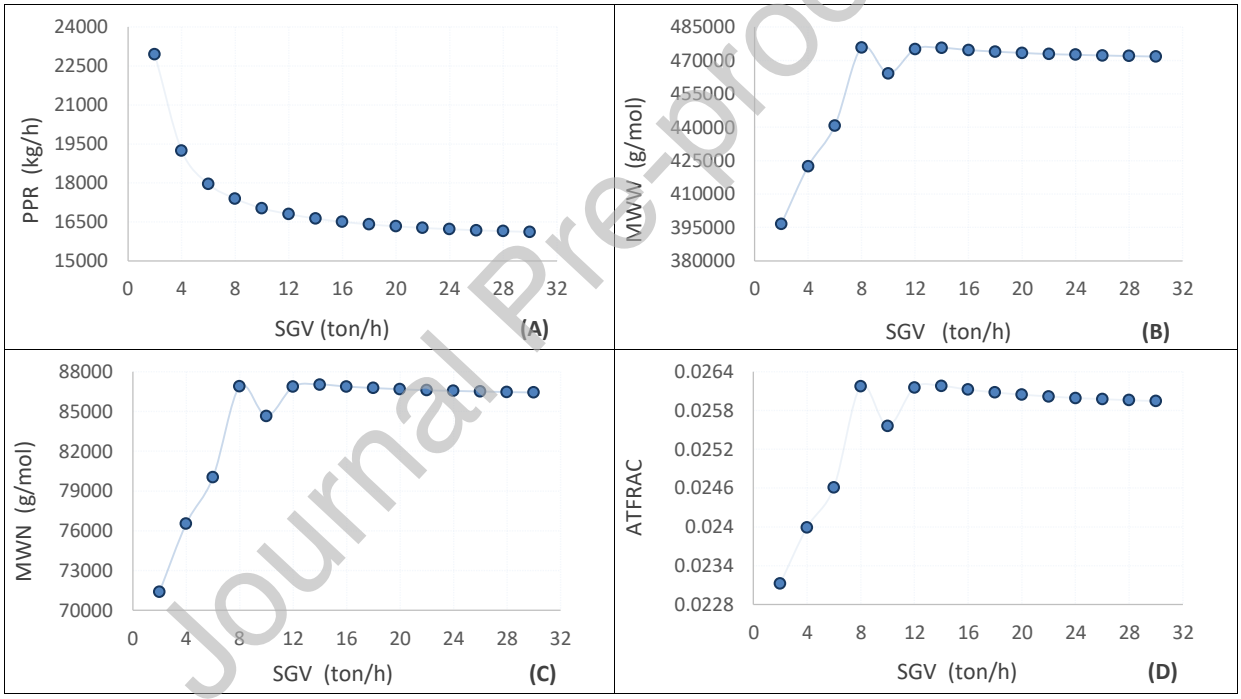

Fig. 17. Effect of SGV on: **A**-propylene production rate; **B**-polymer weight average molecular weight; **C**-polymer number average molecular weight; **D**-polymer atactic fraction.

3.1.4 Hydrogen

Hydrogen is necessary for controlling the polymer molecular weight and transitioning between the various grades during normal operation. Generally, hydrogen reacts with

hindered methyl groups adjacent to propylene and activates them for the propagation reactions (Skoumal, 2007; Dehghani, 2012). In addition, hydrogen may reactivate the sites deactivated by compounds like metalallylics. Despite the differences between the conversion profile through the bubble and emulsion phases (Fig. 18), increasing the inlet hydrogen flow leads to higher overall propylene conversion inside the FBR (Fig. 19A). The decrease in the propylene conversion with hydrogen flow, which appears through the bubble phase, happens because of the varied saturation influence of hydrogen on active sites. Hydrogen may enhance the blocking and de-blocking of active centers by mis-inserted monomer units. Furthermore, this mis-insertion triggered by hydrogen acceleration inside the reactor results in that some of catalytic sites may become temporarily inactive due to steric hindrance. Thus, hydrogen will participate in chain transfer reaction on these blocked (dormant) sites and make them free for further reaction. Since the catalyst concentration in the bubble phase is lower compared to the emulsion phase, the concentration of blocked sites becomes very high in the bubble phase where hydrogen merely plays its main role, which is chain transfer reaction.

As outlined above, hydrogen in the polymerization system acts primarily as a very active chain transfer agent at higher concentrations. Therefore, the polymer molecular weights (MWW and MWN) and viscosity decrease with the hydrogen flow (Fig. 19B and C, respectively). The hydrogen influence on MWW is higher than other variables, especially when the hydrogen percentage in the recycle gases is less than 0.027 vol.% (1100 kg/h). Regarding the steroespecifity, the hydrogen quantity inside the FBR does not seem to have a direct effect on the atactic propagation. However, the higher hydrogen rates inside the FBR cause a decrease in the atactic ratio of the polymer (Fig. 19D). This decrease is elucidated through a competition exists between activation by hydrogen and mis-insertion of irregular monomer inside the aspecific sites, which ultimately affects the atactic propagation rate.

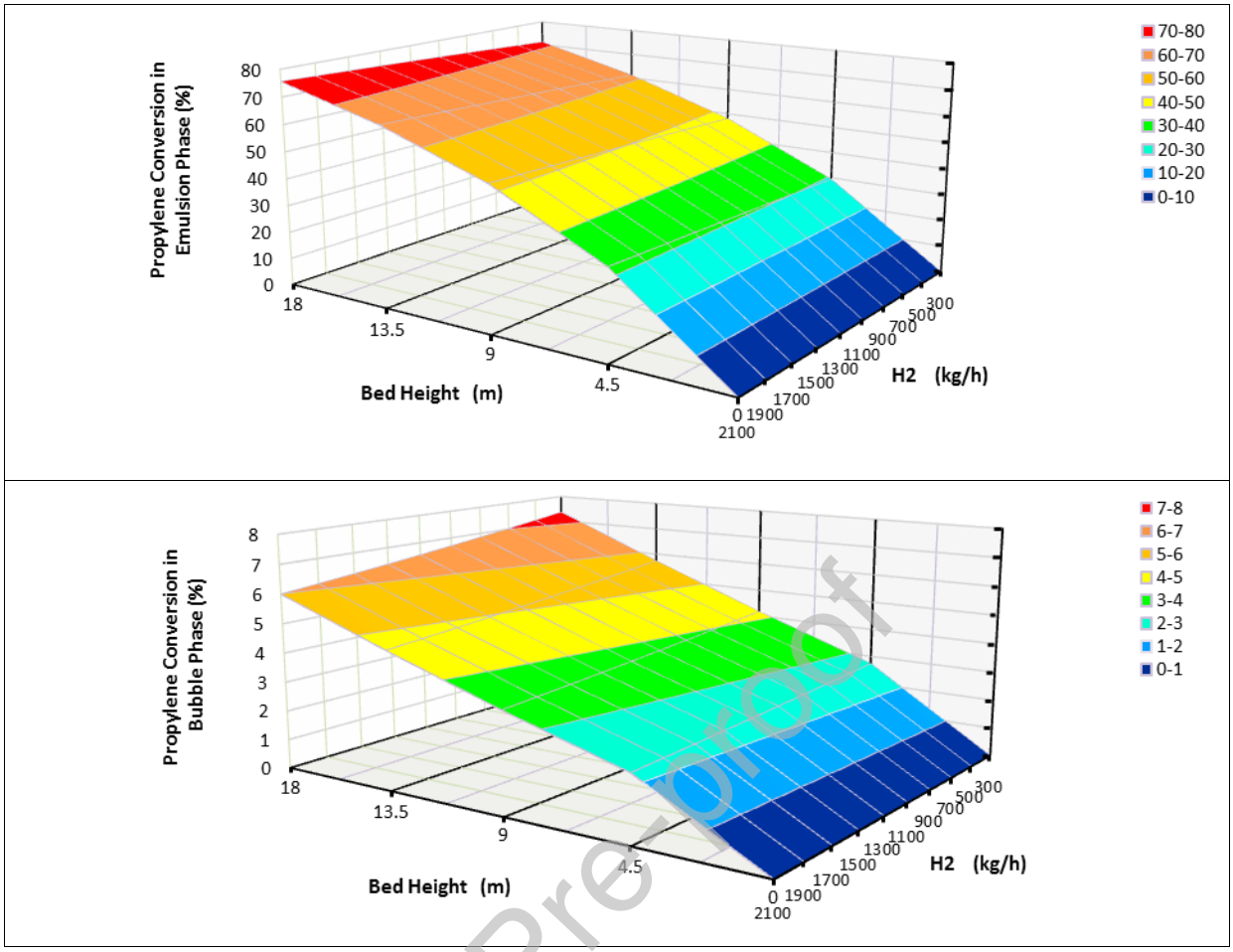

Fig. 18. Variation of FBR propylene conversion through the fluidized bed with hydrogen.

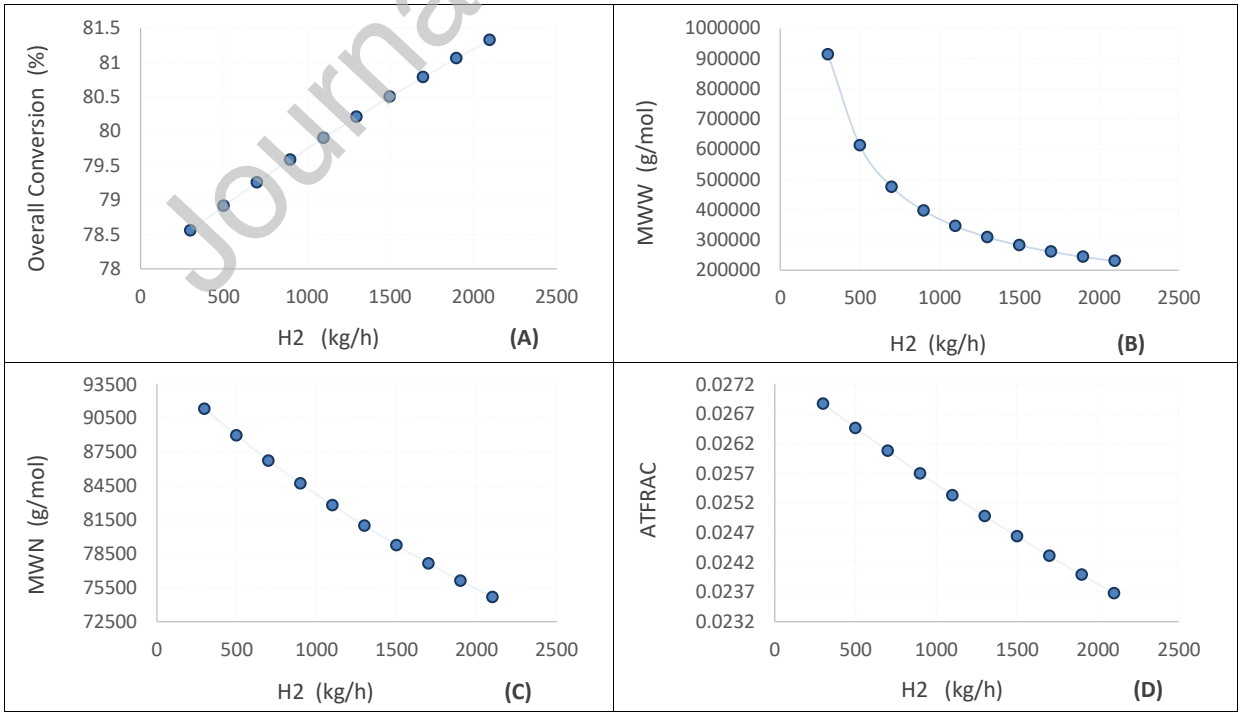

Fig. 19. Effect of hydrogen on: **A**-overall propylene conversion; **B**-polymer weight average molecular weight; **C**-polymer number average molecular weight; **D**-polymer atactic fraction.

3.1.5 Cocatalyst

Cocatalyst plays a reducing role to activate the catalyst through the alkylation, eliminates the halogen atoms from the catalyst, and transfer alkyl group to it. Then, the catalyst site becomes cationic and need to be stabilized. Therefore, the electron–deficient site of the catalyst is ready to absorb the π-electrons of the olefin double bond, making the transferred alkyl group of cocatalyst one of the polymer chain ends (Skoumal, 2007; Soga and Shiono, 1997; Dehghani, 2012). Although the main role of cocatalyst is to activate the catalyst, it also acts as a scavenger of polar impurities and as a chain transfer agent like hydrogen or monomer. Generally, the cocatalyst has a little influence on the polymerization system, inasmuch as the chain propagation is indeed related to the amount of titanium in the catalyst. Hence, a further increase in the amount of cocatalyst slightly increases the activity of chain propagation and hence the production rate inside the FBR (Fig. 20A). The role of cocatalyst as chain transfer agent remarkably appears at higher flow rates, causing an increase in the activity of chain transfer to monomer and hydrogen, thus the polymer molecular weights (MWW and MWN) decrease as shown in Fig. 20B and C, respectively. Meanwhile, as the cocatalyst flow rate increases, the atactic propagation rate increases as shown in Fig. 20D. This is because cocatalyst inhibits the deactivation effect of SCA for aspecific sites, leading to a slight decrease in the degree of the polymer crystallinity.

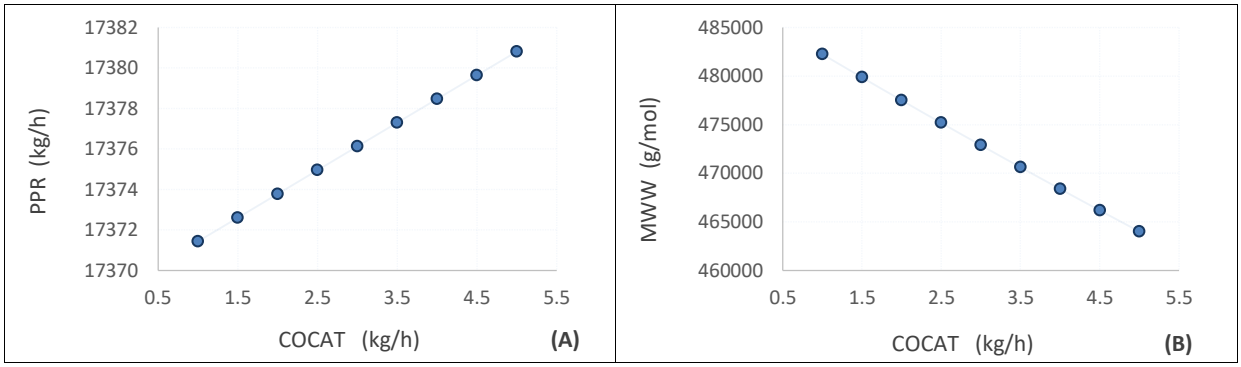

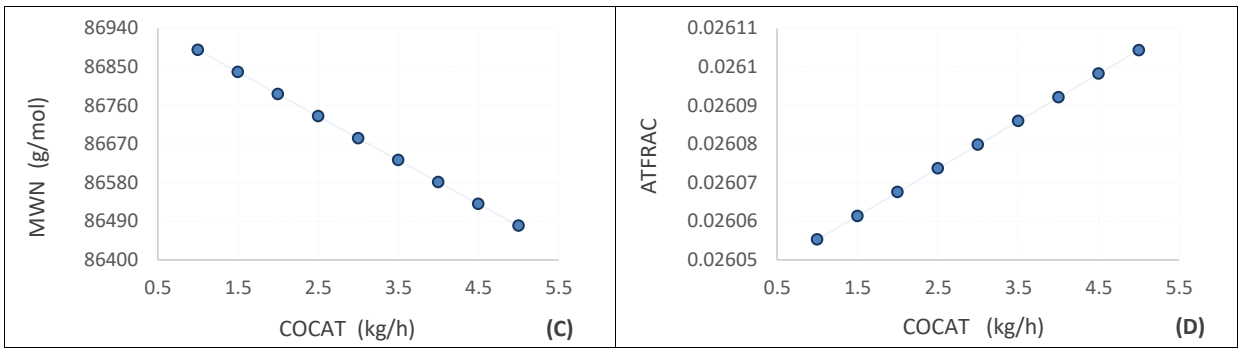

Fig. 20. Effect of cocatalyst flow rate on: **A-** propylene production rate; **B-**polymer weight average molecular weight; **C-**polymer number average molecular weight; **D-**polymer atactic fraction.

3.2 Process improvement

From the previous analysis, it can be concluded that SGV is the dominant operating variable in the whole Unipol® process. The significance of this parameter comes from that it is a main controller in the entire process, especially the fluidization regime inside industrial FBRs. As stated earlier, the superficial gas velocity, not only affects the energy consumption required for fluidizing, but also affects the cooling duty required per monomer mass (direct influence). The net power requirement of the compressor increases with increasing SGV, but the cooling duty of the water cooler decreases (Fig. 21A). As a result of the SGV effect on the thermal gradient along the FBR bed height, the SGV affects the monomer conversion per pass as well as the compression polytropic efficiency. Therefore, the monomer conversion decreases with increasing SGV, while the compression efficiency increases (Fig. 21B). On the other hand, it should be stated here that process improvement/optimization was not implemented in the previous Aspen Plus® models (Luo et al., 2009; Khare et al., 2004; Zheng et al., 2011; Shamiria et al., 2012), inasmuch as most of these models were unable to investigate the influences of SVG, the most dominant process variable.

Other important variables inside the FBR are the COCAT:CAT and COCAT:SCA ratios. As mentioned before, the variation of these ratios leads to the change in the plant productivity

as well as the produced polymer specifications, especially the degree of crystallinity. By varying these ratios, the plant operators usually try to maximize their unit productivity while maintaining the product quality and the safe operation mode inside the FBRs.

As a rule of thumb to avoid the melting and agglomeration of polymer particles inside industrial FBRs, the FBR should operate below the maximum safe bed-operational temperature, at which the bed does not undergo the thermal runaway. Therefore, the top temperature of FBRs present in industrial propylene polymerization units should not exceed the accepted safe limit of 80 ^{o}C (Shamiri et al., 2011). Actually, higher SGVs reduce these risks inside FBRs, making them the preferred conditions for most FBR operators. However, this leads to higher energy consumption and lower production rate. Therefore, access to the optimal SGV is a major priority during normal operation. In addition, the safe range of systematic variation for the main operating parameters such as COCAT:CAT and COCAT:SCA mass ratios should be implemented while maintaining an acceptable margin of the industrial safety limit of 80 ^{o}C to provide the sufficient period for energizing the killing system during emergency accidents to stop the thermal runaway inside the FBR without exceeding this critical temperature.

Before improving a chemical process, two operational scenarios should be confronted: What if a change happened to one or more of the process variables?" and "How to maximize profits?". Many efforts are always performed in order to find solutions for facing "What-if" and "How-to" challenges. Both rigorous analysis of process performance and applying corrective adjustments to actual operation are crucial for improvement/optimization studies. Therefore, this scenario has been executed in the preceding analysis of operating variables. On the other hand, maximizing the profit for an industrial plant is usually an imperious desire. However, this challenge faces veritable obstacles that should be overcome during process improvement.

To improve the process, the notes obtained from the first scenario (analysis of FBR operating variables) should be implemented. The investigated industrial FBR operates currently at the conditions exhibited in Table 9. It is observed that the turbulent regime is the predominant fluidization regime inside the FBR, not the well-mixed regime. Fig. 22 displays the improvement procedures implemented in this study. As indicated, the process improvement begins with the most dominant process variable, SGV. Since the priority of process improvement is to maximize the plant productivity, the first step is to estimate the optimal SGV that fulfills the optimum temperature distribution through the FBR cycle, according to the propylene conversion and the compressor efficiency. The optimal SGV is determined by intersecting the propylene conversion curve with the compressor efficiency curve as illustrated in Fig. 21B. However, the constraint of the ceiling temperature inside the FBR (80 ^{o}C) should be considered. If the optimal velocity cannot fulfill the process constraint, then moving on to the second step is essential. In this step, the optimal SGV that accomplishes the optimum utility and energy consumption through the FBR cycle, according to the water cooler duty and the gas compressor power requirements, is estimated by the intersection of both curves displayed in Fig. 21A. The cooling duty for different SGVs is expressed by the maximum temperature within the FBR (outlet temperature), while the compression duty for different SGVs is represented by the outlet temperature of the compressor, which compensates the pressure drop (ΔP =1 bar) required for fluidizing the recycle gases with a reference mass flow through the bed. After the optimal SGV estimation, the third step for optimizing COCAT:CAT and COCAT:SCA mass ratios is performed. In this step, these ratios are altered simultaneously at the optimal SGV to fulfill a maximum yield of the polymer with identical specifications and to minimize the operating costs of the investigated unit, while retaining an adequate margin of the industrial safety limit inside the FBR.

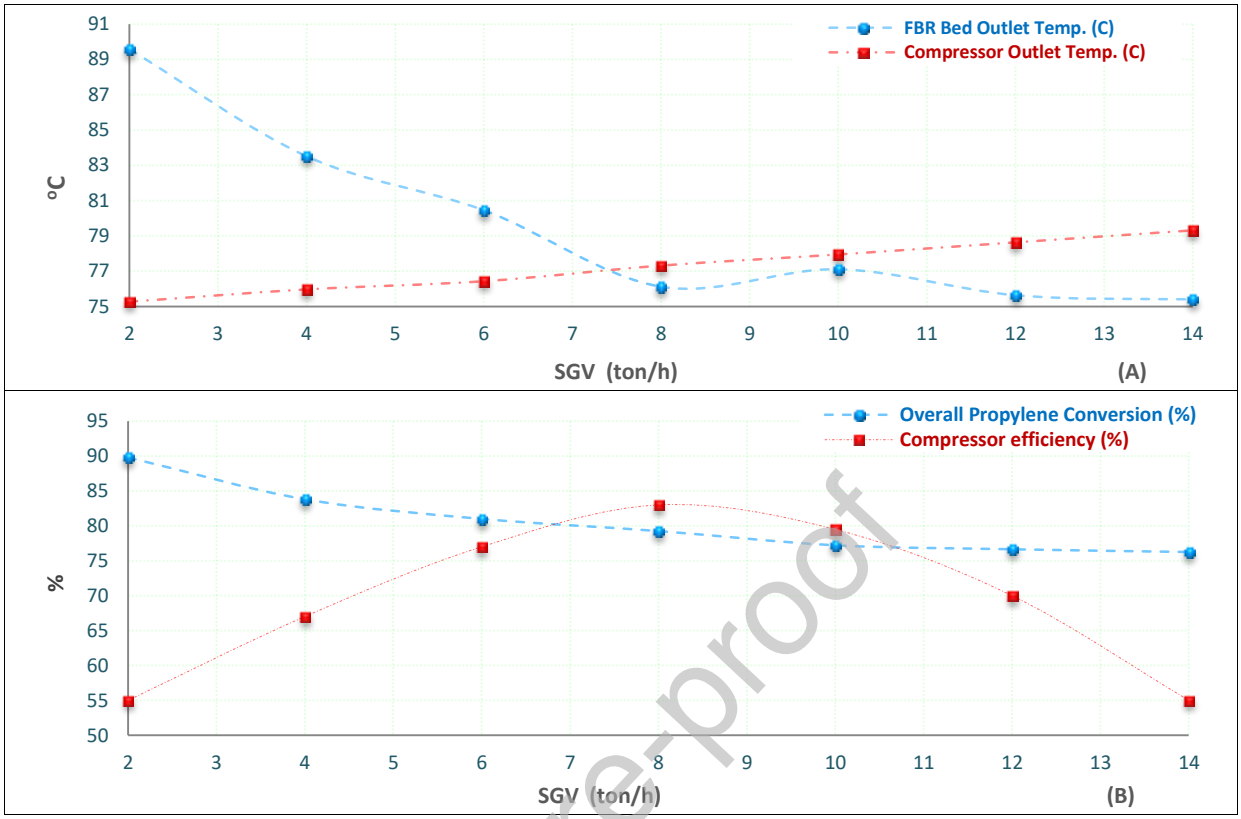

Fig. 21. Effect of SGV on: **A**-FBR bed outlet temperature and recycle gas compressor outlet temperature; **B**-overall propylene conversion and recycle gas compressor efficiency.

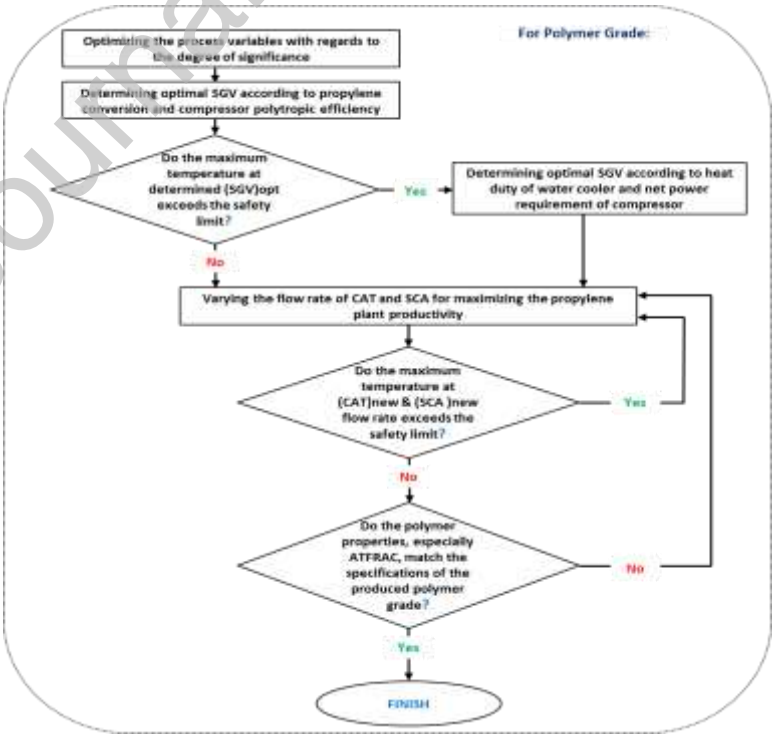

Fig. 22. Improvement methodology implemented in the current study.

The improved operating conditions are listed in Table 9, whereas the results of the improvement are shown in Tables 10 and 11. About 1,436 kg/h can be added to the polypropylene yield, while maintaining the produced polymer specifications, by following the suggested optimization scheme. Savings in the polypropylene yield are mainly attributed to the increase in the polymerization reactions activity inside the FBR through applying the optimum scheme. Since the optimal SGV is lower compared to the base fluidization velocity, approximately 29.5 kW can be saved from the recycle gas compressor. It should be emphasized that the optimal SGV generally represents the optimum operating conditions that fulfill the highest production rate with the lowest operating costs. The improved scheme can attain additional annual profits in excess of USD 15 million for the investigated unit, according to the global marketing value of the product during the study period, thereby more profits for the plant operators. It should be pointed out here that saving in the energy and product yield are primarily proportional to plant capacity.

Table 9. Operating conditions of the unit at the base point and at the improved point.

Process Variable	**Base Operating Point**	**Improved Operating Point**
SGV [ton/h]	8.15	7.6
COCAT:CAT mass ratio	3.671	3.338
COCAT:SCA mass ratio	1.436	1.46

Table 10. Variation in plant performance after applying the improved scheme.

Parameters	**Before Improvement**	**After Improvement**	**Differences**
Plant operating variables:			
Compressor horsepower required [kW]	466.9	437.4	-29.5
Plant productivity:			
Polypropylene [kg/h]	17,375	18,811	+1,436

Table 11. Variation in grade SB-25 specifications after applying the improved scheme.

Product SB-25 Specifications	Before Improvement	After Improvement	Limits
MFI [g/10 min]	1.5	1.62	1.5 min - 2.1 max
ATFRAC [mol.%]	2.6	2.7	2 min - 2.8 max
PDI	5.72	5.68	4 min - 7 max

Finally, the model can be utilized to forecast the plant performance at different operating points, inasmuch as it represents the actual fluidization regime of the fluidized bed within the plant FBR. The model is quite useful for on-line prediction of proper operating conditions, especially when the unit suffers during the transition between polymer grades. This may be executed by incorporating the model into a real-time optimization scheme. In this case, it is recommended that the model be finely tuned as implemented in the current study to correspond with the plant performance strictly.

4. Conclusions

A two-phase process model for an industrial gas phase polypropylene process based on Unipol® technology was developed by applying the fundamental engineering principles concluded from the literature and using the advanced Aspen Plus software tools. Because of the difficulty in simulating the FBR by commercial software, the built-in SMS approach with the hydrodynamic correlations deduced from the previous studies were applied. The combination between standard modules available in Polymers Plus® library is considered a logic way to dazzlingly represent the real hydrodynamic behavior inside industrial FBRs. Through SMS approach, the fluidized bed of the plant FBR was modeled as operating in its actual fluidization state, i.e. in turbulent regime. An advanced technique for developing and calibrating the industrial Unipol® process model, different from other techniques

implemented in the previous studies, was applied. The model could track the plant performance competently. Thus, the model was utilized for investigating the effect of each process variable on the process performance. Among all process variables, SGV was the most dominant factor to influence the process performance. The model was used for improving the process at steady-state conditions. Results acquired from the model showed that a considerable increase in the polypropylene yield, while maintaining the produced polymer specifications, could be achieved by optimizing SGV while adjusting COCAT:CAT and COCAT:SCA mass ratios. Applying the improvement scheme saves the plant consumption of energy as well as enhances the plant productivity. The model developed here can be also utilized to explore and analyze the dynamic performance of the FBR control system. Finally, the model can also be integrated into a real-time optimization scheme to continuously attain the optimal conditions during the plant operation. In this situation, the model should be finely tuned as executed in the current study to coincide in the plant performance strictly.

Author Contribution Statement

Eslam S. Sbaaei: Methodology, Investigation, Formal analysis, Software, Validation, Writing - Original Draft, Visualization

Mai M. Kamal Fouad: Conceptualization, Methodology, Formal analysis, Validation, Writing - Review & Editing, Visualization, Supervision

Tamer S. Ahmed: Conceptualization, Methodology, Formal analysis, Validation, Writing - Review & Editing, Visualization, Supervision

Nomenclature

A_s	Sphere area (m^2)
A_p	Particle area (m^2)
$DCAT_i$	Deactivated catalyst site of type *i*
D_n	Inactive polymer chain with n monomer segments
d_p	Solid particle diameter (m)
$k_{act,i}$	Rate constant for activation of catalyst site type *i* by cocatalyst
$k_{ds,i}$	Rate constant of spontaneous deactivation for catalyst site type *i*
$k_{dsca,i}$	Rate constant for deactivation of catalyst site type *i* by SCA
$k_{ini,i}$	Rate constant for chain initiation of catalyst site type *i*
$k_{p,i}$	Rate constant for chain propagation of catalyst site type *i*
$k_{pa,i}$	Rate constant for chain propagation of catalyst site type *i*
$k_{sp,i}$	Rate constant for spontaneous activation of catalyst site type *i*
$k_{tco,i}$	Rate constant for chain transfer to cocatalyst attached to catalyst site type *i*
$k_{th,i}$	Rate constant for chain transfer to hydrogen attached to catalyst site type *i*
$k_{tm,i}$	Rate constant for chain transfer to monomer attached to catalyst site type *i*
$P_{0,i}$	Activate catalyst site of type *i*
$P_{1,i}$	Initiated catalyst site of type *i*
$P_{n,i}$	Live polymer chain with n segments attached to catalyst site of type *i*
T_{ref}	Reference temperature (K)
U_{mf}	Minimum fluidization velocity (m/s)
U_0	Actual fluidization velocity (m/s)
w_j	Weighting factor of process variable j
X_j	Process variable j

Abbreviations:

ACT-COCAT	Catalyst activation by cocatalyst reaction
Act-Energy	Activation energy

ACT-SPON	Catalyst spontaneous activation reaction
ATACT-PROP	Atactic propagation reaction
ATFRAC	Atactic fraction
BOBYQA	Bound Optimization BY Quadratic Approximation
C3H6-R	Propylene segment
CAT	Catalyst
CHAIN-INI	Chain initiation reaction
CHAT-COCAT	Chain transfer to cocatalyst reaction
CHAT-H2	Chain transfer to hydrogen reaction
CHAT-MON	Chain transfer to monomer reaction
COCAT	Cocatalyst
CSTR	Continuous stirred-tank reactor
DEACT-EDONOR	catalyst deactivation by SCA reaction
DEACT-SPON	Spontaneous catalyst deactivation reaction
FBR	Fluidized bed reactor
RF-03/05	Raffia grade
FM-03	Film grade
GPC	Gel Permeation Chromatography
H2	Hydrogen
M	Monomer
MFI	Melt flow index
MWW	Weight average molecular weight
MWN	Number average molecular weight
N2	Nitrogen
PC-SAFT	Perturbed chain-statistical associating fluid theory
PDI	Polydispersity index
PFR	Plug flow reactor

PPR	Polypropylene production rate
Pre-Exp	Pre-exponential factor
PROPAGATION	Chain propagation reaction
Rxn-Type	Reaction type
SB-25	Spun bond non-woven fabric grade
SCA	Stereospecific control agent
SHAC®	Super high activity catalyst
SMS	Sequential modular simulation
SVG	Superficial gas velocity
TABA	Tertbutyl peroxybenzoate
TEAL	Triethyl aluminum
Z-N	Ziegler-Natta

Greek letters:

Δt	Thermal rise or drop
ρ_g	Gas density
ρ_s	Solid particle density
ρ_c	Catalyst density
μ	gas viscosity
δ_B	Bubble phase fraction
η	Mass transfer driving force
Ψ	Sphericity
ε_{mf}	Porosity at minimum fluidization

5. References

Abbasi, M.R., Shamiri, A., Hussain, M.A., 2016. Dynamic modeling and Molecular Weight Distribution of ethylene copolymerization in an industrial gas-phase Fluidized-Bed Reactor. Adv. Powder Technol. 27, 1526–1538. https://doi.org/10.1016/j.apt.2016.05.014

Ashrafi, O., Mostoufi, N., Sotudeh-Gharebagh, R., 2012. Two phase steady-state particle size distribution in a gas-phase fluidized bed ethylene polymerization reactor. Chem. Eng. Sci. 73, 1–7. https://doi.org/10.1016/j.ces.2012.01.018

Biron, M., 2018. The Plastics Industry: Economic Overview, in: Thermoplastics and Thermoplastic Composites. William Andrew Publishing, pp. 31–132. https://doi.org/10.1016/b978-185617478-7.50008-8

Choi, K.Y., Ray, W.H., 1988. The dynamic behavior of continuous stirred-bed reactors for the solid catalyzed gas phase polymerization of propylene. Chem. Eng. Sci. 43, 2587–2604. https://doi.org/10.1016/0009-2509(88)80003-4

Cui, H., Mostoufi, N., Chaouki, J., 2000. Characterization of dynamic gas-solid distribution in fluidized beds. Chem. Eng. J. 79, 133–143. https://doi.org/10.1016/S1385-8947(00)00178-9

Dehghani, S.S., 2012. Study of ethylene / propylene polymerization , using a 4th generation Ziegler-Natta catalyst : Effect of external donor and feed ratio on polymerization. Chemical Engineering, University of Waterloo: M.Sc. Thesis.

Gross, J., Sadowski, G., 2001. Perturbed-chain SAFT: An equation of state based on a perturbation theory for chain molecules. Ind. Eng. Chem. Res. 40, 1244–1260. https://doi.org/10.1021/ie0003887

Hatzantonis, H., Yiannoulakis, H., Yiagopoulos, A., Kiparissides, C., 2000. Recent developments in modeling gas-phase catalyzed olefin polymerization fluidized-bed reactors: The effect of bubble size variation on the reactor's performance. Chem. Eng. Sci. 55, 3237–3259. https://doi.org/10.1016/S0009-2509(99)00565-5

Ibrehem, A.S., Hussain, M.A., Ghasem, N.M., 2009. Modified mathematical model for gas phase olefin polymerization in fluidized-bed catalytic reactor 149, 353–362. https://doi.org/10.1016/j.cej.2008.05.014

Jafari, R., Sotudeh-gharebagh, R., Mostoufi, N., 2004a. Full Papers Modular Simulation of Fluidized Bed Reactors. Chem. Eng. Technol. 27, 123–129. https://doi.org/10.1002/ceat.200401908

Jafari, R., Sotudeh-Gharebagh, R., Mostoufi, N., 2004b. Performance of the wide-ranging models for fluidized bed reactors. Adv. Powder Technol. 15, 533–548. https://doi.org/10.1163/1568552042000192

Khare, N.P., Seavey, K.C., Liu, Y.A., Ramanathan, S., Lingard, S., Chen, C.C., 2002. Steady-state and dynamic modeling of commercial slurry high-density polyethylene (HDPE) processes. Ind. Eng. Chem. Res. 41, 5601–5618. https://doi.org/10.1021/ie020451n

Khare, N.P., Lucas, B., Seavey, K.C., Liu, Y.A., Sirohi, A., Ramanathan, S., Lingard, S., Song, Y., Chen, C.C., 2004. Steady-State and Dynamic Modeling of Gas-Phase Polypropylene Processes Using Stirred-Bed Reactors. Ind. Eng. Chem. Res. 43, 884–900. https://doi.org/10.1021/ie030714t

Kiashemshaki, A., Mostoufi, N., Sotudeh-gharebagh, R., 2006. Two-phase modeling of a gas phase polyethylene fluidized bed reactor 61, 3997–4006. https://doi.org/10.1016/j.ces.2006.01.042

Kunii, D., Levenspiel, O., 1991. Fluidization Engineering, 2nd ed, wiley. Butterworth-

Heinemann, USA. https://doi.org/10.1016/b978-0-7506-9236-6.50001-9

Luo, Z.H., Su, P.L., Shi, D.P., Zheng, Z.W., 2009. Steady-state and dynamic modeling of commercial bulk polypropylene process of Hypol technology. Chem. Eng. J. 149, 370–382. https://doi.org/10.1016/j.cej.2009.01.021

Maddah, H.A., 2016. Polypropylene as a Promising Plastic : A Review. Am. J. Polym. Sci. 6, 1–11. https://doi.org/10.5923/j.ajps.20160601.01

Mahecha-Botero, A., Grace, J.R., Elnashaie, S.S.E.H., Lim, C.J., 2009. Advances in modeling of fluidized-bed catalytic reactors: A comprehensive review. Chem. Eng. Commun. 196, 1375–1405. https://doi.org/10.1080/00986440902938709

McAuley, K.B., MacGregor, J.F., Hamielec, A.E., 1990. A kinetic model for industrial gas-phase ethylene copolymerization. AIChE J. 36, 837–850. https://doi.org/10.1002/aic.690360605

Mostoufi, N., Cui, H., Chaouki, J., 2001. A comparison of two- and single-phase models for fluidized-bed reactors. Ind. Eng. Chem. Res. 40, 5526–5532. https://doi.org/10.1021/ie010121n

Pashikanti, K., Liu, Y.A., 2011. Predictive Modeling of Large-Scale Integrated Refinery Reaction and Fractionation Systems from Plant Data . Part 2 : Fluid Catalytic Cracking (FCC) Process. Energy & Fuels 25, 5298–5319. https://doi.org/https://doi.org/10.1021/ef200750x

Pasquini, N., 2005. Polypropylene Morphology, in: Polypropylene Handbook. Hanser Gardner Publications, USA&Canda, pp. 147–264.

Sbaaei, E.S., Ahmed, T.S., 2018. Predictive modeling and optimization for an industrial Coker Complex Hydrotreating unit – development and a case study. Fuel 212, 61–76. https://doi.org/10.1016/j.fuel.2017.10.032

Shamiri, A., Azlan Hussain, M., Sabri Mjalli, F., Mostoufi, N., Saleh Shafeeyan, M., 2011. Dynamic modeling of gas phase propylene homopolymerization in fluidized bed reactors. Chem. Eng. Sci. 66, 1189–1199. https://doi.org/10.1016/j.ces.2010.12.030

Shamiri, A., Hussain, M.A., Mjalli, F.S., Mostoufi, N., 2010. Kinetic modeling of propylene homopolymerization in a gas-phase fluidized-bed reactor. Chem. Eng. J. 161, 240–249. https://doi.org/10.1016/j.cej.2010.04.037

Shamiri, A., Azlan, M., Sabri, F., Mostoufi, N., 2012. Improved single phase modeling of propylene polymerization in a fluidized bed reactor. Comput. Chem. Eng. 36, 35–47. https://doi.org/10.1016/j.compchemeng.2011.07.015

Shamiria, A., Hussaina, M.A., Mjallic, F., Mostoufid, N., 2012. Comparative simulation study of gas-phase propylene polymerization in fluidized bed reactors using aspen polymers and two phase models. Chem. Ind. Chem. Eng. Q. 19, 13–24. https://doi.org/10.2298/ciceq111214038s

Skoumal, M., 2007. Characterization of MgCl 2 -supported Catalyst and Initial Kinetics Determination in Low-pressure Propene Polymerization. University of Twente: Ph.D. Thesis, Enschede.

Soga, K., Shiono, T., 1997. Ziegler–Natta Catalysts Polymerizations. Prog. Polym. Sci. 22, 1503–1546. https://doi.org/10.1016/S0079-6700(97)00003-8

Taskar, U., Riggs, J.B., 1997. Modeling and Optimization of a Semiregenerative Catalytic Naphtha Reformer. AIChE J. 43, 740–753. https://doi.org/10.1002/aic.690430319

Zheng, Z.W., Shi, D.P., Su, P.L., Luo, Z.H., Li, X.J., 2011. Steady-state and dynamic modeling of the Basell multireactor olefin polymerization process. Ind. Eng. Chem. Res. 50, 322–331. https://doi.org/10.1021/ie101699b

GRAPHICAL ABSTRACT

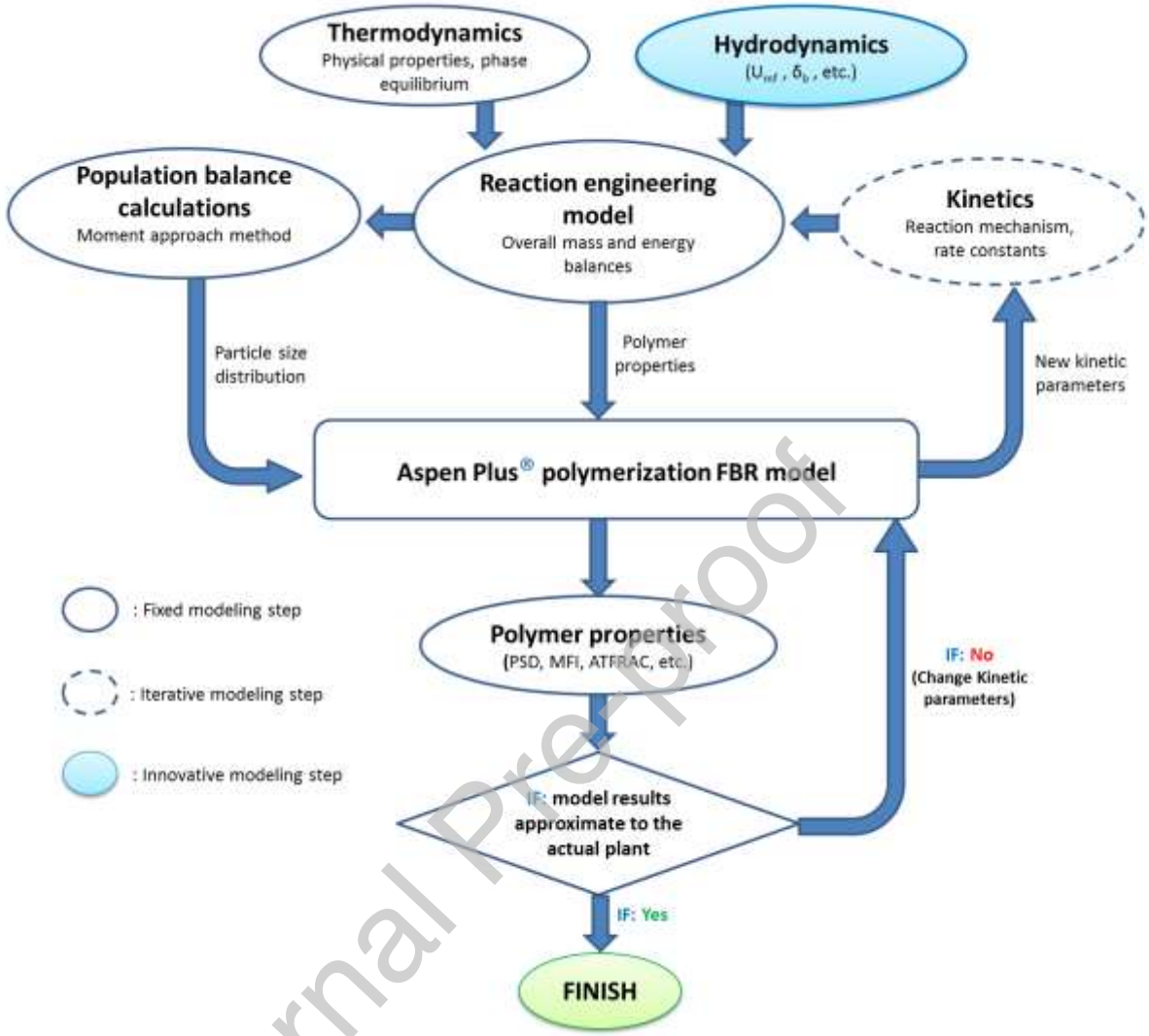

Declaration of interests

☒ The authors declare that they have no known competing financial interests or personal relationships that could have appeared to influence the work reported in this paper.

☐The authors declare the following financial interests/personal relationships which may be considered as potential competing interests: